QUADRUPOLE MASS FILTER DESIGN

AND CONSTRUCTION FOR

PLASMA ION ANALYSIS

By

HAROLD WAYNE WILLIS

Bachelor of Science

Lamar State College of Technology

Beaumont, Texas

1966

Submitted to the Faculty of the Graduate College
of the Oklahoma State University
in partial fulfillment of the requirements
for the degree of
MASTER OF SCIENCE
August, 1969

730178

730178

QUADRUPOLE MASS FILTER DESIGN

AND CONSTRUCTION FOR

PLASMA ION ANALYSIS

Thesis Approved:

Francis C. Todd
Thesis Adviser

Leon W. Schroeder

Tom E. Moore

E. E. Kohnke

N. N. Durham
Dean of the Graduate College

PREFACE

Under the direction of Dr. F. C. Todd, the major advisor to
this student, a quadrupole mass filter has been designed and is
presently in use as an analytical tool for measuring properties of
transient aluminum plasmas.

This device has been employed to determine the presence of
different ionic species in a dense aluminum plasma produced by a
spark gap in vacuum. It has also been used to some extent to study
the velocity distribution of the plasma ions.

The student is grateful for the preliminary work done on this
project by Mr. Larry J. Peery and for the many hours of consulta-
tion with Mr. William G. Robinson. For assistance in the design and
contruction of the electronic components, many thanks are due Mr.
John F. Stoops. Mr. Heinz Hall and Mr. M. Wayne Atkins were respon-
sible for much of the construction of the quadrupole vacuum system.

Without the assistance and guidance of Dr. Todd, the completion
of this work would have been impossible.

The understanding patience and the unselfish assistance of my
wife, Eva, in typing the manuscript have been invaluable in the pre-
paration of this work. The kindly restraint of Misty in providing
a studious atmosphere at home has been greatly appreciated.

TABLE OF CONTENTS

LIST OF TABLES

LIST OF FIGURES

vi

CHAPTER I

INTRODUCTION

One of the oldest disciplines in science is the field of electrical discharges in gases. Sir William Crookes, in 1879, considering the special properties of the matter in discharge tubes, tentatively advanced the idea that these excited gases should be considered a fourth state of matter. Compton and Langmuir (1930) introduced the special designation "plasma". Descriptively, the term simply denotes ionized gases. Depending on the degree of ionization, such gases exhibit similarities to metals, semiconductors, strong electrolytes and ordinary gases. The concept "fourth state of matter" thus derives from the extraordinary array of physical and chemical properties characteristics of a plasma. This classification is usually reserved for those cases wherein the densities of charges of each sign are approximately equal, i.e., the cases for which quasi-neutrality exit (Hellund, 1961).

Another source similarly defines the plasma as an electrically charged gas consisting of ions and electrons. It is therefore an electrical conductor. The distinction between a liquid conductor and a plasma is not very precise and can be most easily made in terms of particle densities. When speaking of a liquid conductor, one is usually talking in terms of the order of 10^{22} charged particles per cubic centimeter. When the term plasma was first applied, the number

of charged particles was of the order of 10^{18} and lower and neutral atoms were always present (Gartenhaus, 1964). A plasma may be thought of as a gaseous conductor. Neutral atoms are always present since plasmas emit light with the recombination of ions and electrons, and light is always emitted. This is experimentally verified by recording the emission of the characteristic radiation. A spectral analysis with a far ultraviolet spectrograph was made of the light from the breakdown of a spark gap in a vacuum. This spectra definitely shows that metastable atoms are present in the plasma (Carpenter, 1967). The presence of the neutrals has been further verified by the qualitative measurements taken with the quadrupole mass filter. This device was used to analyze both the vacuum spark gap breakdown and the laser impact in which aluminum was the principle plasma producing source.

The Plasma Group at Oklahoma State University, conducted by F. C. Todd, has concentrated its efforts on the study of transient, dense aluminum plasmas. The facilities for producing this type of plasma consist of essentially the following:

    (1) A Q-switched, twin ruby rod laser

    (2) An exploding wire device

    (3) A device to induce the vacuum breakdown of the gap be-
           tween spectroscopically pure aluminum electrodes

The laser is capable of delivering a tremendous energy output to a relatively small target area in a very short time interval so that peak power outputs of the order of 0.33×10^{9} watts have been attained. This power is used to create and sustain an aluminum plasma long enough for experimental investigations to be made.

The exploding wire facility produces a plasma by a pulse of

power with a duration of one microsecond. (This period is not to be confused with the life time of the plasma itself). This should enhance the resolution with which further velocity distribution investigations may be made. The device consist essentially of a vacuum chamber, into which is placed a short aluminum wire of one one-thousandth inch diameter. A high voltage power supply (100 KV) is used to drive a one microsecond pulse along a co-axial cable, which terminates in the small aluminum wire. The characteristic impedance of the cable is 50 ohms so a peak current of the order of 2,000 amperes is expected. The ambient resistance of the target wire is approximately 1.4 ohms, with an estimated average resistance during the pulse of five times this amount, or 7.0 ohms. The peak power input to the plasma could possibly attain a value of 28×10^6 watts; however, the total energy into the plasma is only 28 watt-seconds (joules).

The vacuum spark gap apparatus consist of a vacuum envelope with a glass manifold. With the use of mechanical feedthroughs, the spectroscopically pure aluminum electrodes are positioned so that a gap width of the order of 1.0 mm is obtained. By means of the manifold on the vacuum envelope, a pulsed photomultiplier may be employed to monitor the visible and the ultraviolet light emission. A high voltage power supply is used to charge a 12.5 KV condenser, which is then allowed to discharge across the gap. The very high potential gradients at the electrode points causes a breakdown of the spark gap. The high current density arc at breakdown produces ions and electrons which, in fact, comprise the plasma. The light emission results from the downward transitions in the ionized, or excited atoms.

The analytical tools for investigating the properties of the

aluminum plasmas mentioned in the text above may be summarized by the following:

(a) A vacuum spectrograph for the far ultaviolet (Payne, 1966).

(b) A pulsed, high gain photomultiplier to record the intensity variation with time for a fraction of the visible plus the ultraviolet light emission (Brown, 1968)

(c) The quadrupole mass filter

The purpose of this thesis is fourfold. [1]A description is given of the design and construction of the quadrupole mass filter. [2]The results of the preliminary investigations of the spark discharge and laser impact are presented. [3]The analytical study, the design and the construction details of a pulsed electrostatic lens are presented. This lens is to be used in conjunction with the quadrupole mass filter to study ion velocities. [4]Improvements on existing methods and equipment for future investigations are suggested.

CHAPTER II

THEORETICAL DISCUSSION

Mass - Spectrometer Development

Since 1913, when J. J. Thomson developed the parabolic mass -
spectrometer employing parallel electrostatic and magnetic fields,
many techniques have been developed for mass analysis as is apparent
through examination of the literature (Mosharrafa, 1961). The most
common types of mass - spectrometers are:

    (1) The Magnetic mass - spectrometer

    (2) Time-of-flight mass - spectrometer

    (3) The Quadrupole - type spectrometer

The magnetic mass - spectrometer analyzes the mass of mono-
energetic ion beams by using 60°, 90° or 180° homogeneous sector
magnetic fields. In fact, sector fields up to five revolutions of
360° have been successfully used.

The time-of-flight mass - spectrometer utilizes the principle
that the time needed for an ion with specific energy to traverse a
drift space is dependent on the ionic mass.

A rather new type of mass - spectrometer was developed by W.
Paul and others (1955) at the University of Bonn, Germany, since
1953. This spectrometer employs the "mass filtering" principle
which concerns the ejecting of ions through a quadrupole rf field,
with a dc field applied simultaneously.

5

This quadrupole mass-spectrometer or mass filter, as it may be more appropriately named, was chosen for the particular applications in this plasma group for a variety of reasons:

(1) The resolution of the instrument is variable and can be changed very easily by simply changing the ratio of the applied dc voltage to the rf voltage amplitudes. This makes it possible to insure maximum efficiency and hence, higher sensitivity throughout the entire mass range. It should be noted, however, that for the application to the work reported here, only the single mass of aluminum (13) has been of interest.

(2) Contrary to the other two types of spectrometers mentioned above, the quadrupole mass filter offers no velocity discrimination, i.e., the device will monitor ions of whatever velocity, so long as an upper limit is not exceeded. (This point will be further explained later in the text.)

(3) The quadrupole requires no type of magnetic field. It is well known that stray magnetic fields greatly disturb the conditions of an active, as well as a passive plasma. This eliminates, almost entirely, the difficult shielding problems which plague the magnetic spectrometers.

(4) A very tolerable acceptance angle of 30° reduces, considerably, the necessity for entrance and exit slits and other complicated focusing and collimating requirements.

(5) An extra feature of being bakable insures the attain-

ability of a clean, high vacuum system.

The very nature of the transient plasmas that were produced in this investigation required that a detection system, coupled with the mass filter, be useful for fast scanning purposes. There are several methods available for ion detection and a few of them may be listed as an indication of the scope of endeavor in this research area:

Detector Systems

(1) Farady cup: This method has an advantage of a high collection efficiency because of the large coverage space of the collector. However, it is much less sensitive than some of the other types and must be coupled with an electrometer or other similar instrument to detect small ion currents of the order of 10^{-12} Amperes.

(2) Electron Multiplier - Oscilloscope: This method combines the use of an electron multiplier, which amplifies the ion current through secondary electron emission gain, with an oscilloscope, which is triggered by the multiplier output.

(3) Electron Multiplier - Electrometer - Recorder: In this method the current output from the multiplier is integrated, using a vibrating reed type electrometer. The signal is then recorded on a strip chart recorder.

Although there are several other methods of ion current detection, they are easily available in the current literature.

The electron multiplier - oscilloscope method was chosen because it is a very fast detection system. In addition, the high gain of the multiplier makes possible a reasonable oscilloscope display, which may be photographed as a permanent record of the output.

With the plasma - producing equipment being available, and with the choice of the ion analyzer and detector system having been made, the theory of such an instrument and its principle of operation can now be given.

Quadrupole Theory

A literature search by L. J. Peery (1967) proved to be fruitful, in that a wealth of reference material (Brubaker and Tuul, 1964; Woodward and Crawford, 1963) has been compiled which illustrates the adaptability and widening use of the quadrupole mass filter since its conception by Paul and Steinwedel (1953). Its role varies from a partial pressure analyzer (Gunther, 1960) and residual gas detector, to that of detecting ions in plasma analysis. Although the principle of operation is essentially the same for most of its applications, this report will be restricted to the latter.

The quadrupole mass filter employs electric fields which permit only those ions which have a particular charge-to-mass ratio to pass through it. In theory, all other ions, having a different ratio, are rejected. This mass filtering action is based on the behavior of the solutions of the equations of motion of the injected charged particles or ions.

The application of a voltage ($U + V \cos \omega t$) on a hyperbola-shaped quadrupole, as will be shown later in Figure 4, results in

the establishment of a potential distribution within the quadrupole

region which can be written, neglecting end effects, as

$$\phi = (U + V \cos \omega t) \frac{x^2 - y^2}{r_o^2} \tag{2.1}$$

where: ϕ = electric potential

U = dc voltage

V = rf voltage

ω = driving frequency

r_o = distance from the origin to the point of inter-

section of the hyperbolae with the x and y axes

That this solution results is shown by solving the Laplace

equation for hyperbolic fields.

$$\nabla^2 \phi = 0 \tag{2.2}$$

If we assume a solution,

$$\phi = \phi(t) \ (\alpha x^2 - \beta y^2 + \gamma z^2) \tag{2.3}$$

the substitution of it back into Laplaces' Equation (2.2) yields

the following relation between the constants:

$$\alpha - \beta + \gamma = 0 \tag{2.4}$$

If we consider that the tangential field at the hyperbolic surfaces

is given,

$$(\frac{\partial \phi}{\partial z})_{surface} = 0 \tag{2.5}$$

then

$$\phi(t) \ (2\gamma z) = 0 \tag{2.6}$$

or

$$\gamma = 0 \tag{2.7}$$

Therefore Equation (2.3) becomes

$$\phi = \phi(t) \; (\alpha x^2 - \beta y^2) \tag{2.8}$$

Now apply the equations of the hyperbolic surfaces themselves,

$$\pm \frac{x^2}{r_o^2} \mp \frac{y^2}{r_o^2} = 1 \tag{2.9}$$

to Equation (2.8). Equation (2.4) combined with Equations (2.8) and (2.9) now yields the value of the remaining constants.

$$\alpha = \beta = \frac{1}{r_o^2} \tag{2.10}$$

If the time-dependent field is given,

$$\phi(t) = U + V \cos \omega t \tag{2.11}$$

the potential distribution for the region is then given

$$\phi = (U + V \cos \omega t) \; \frac{x^2 - y^2}{r_o^2} \tag{2.1}$$

as was intended to be shown.

Having obtained the potential distribution, the electric field is then calculated component-wise using the familiar relation,

$$\vec{E} = - \vec{\nabla} \phi \tag{2.12}$$

Hence:

$$E_x = - \frac{\partial \phi}{\partial x} = - 2(U + V \cos \omega t) \; \frac{x}{r_o^2} \tag{2.13}$$

$$E_x = -\frac{\partial \emptyset}{\partial y} = 2(U + V \cos \omega t)\frac{y}{r_o^2} \qquad (2.14)$$

and

$$E_z = 0 \qquad (2.15)$$

It is now desirable to analyze the motion of a positively charged particle which is injected into this time-varying field along the z-axis.

The equations in the x, y and z directions are given according to Newton's second law,

$$\vec{F} = m\,\vec{a} = m\,\vec{\ddot{u}} = Z\,e\,\vec{E} \qquad (2.16)$$

where: u = x, y or z

Z = degree of ionization

e = electronic charge

E = electric field strength

Along the x and y directions, the equations of motion are given, respectively,

$$m\,\ddot{x} = Z\,e\,E_x = -2\,Z\,e(U + V \cos \omega t)\frac{x}{r_o^2} \qquad (2.17)$$

$$m\,\ddot{y} = Z\,e\,E_y = 2\,Z\,e(U + V \cos \omega t)\frac{y}{r_o^2} \qquad (2.18)$$

The motion along the z-axis is simply given,

$$m\,\ddot{z} = 0; \quad m\,\dot{z} = \text{constant} \qquad (2.19)$$

The last equation presents no problem, but for Equation (2.17) and (2.18), consider a change of variables,

$$\zeta = \omega t/2 \qquad (2.20)$$

so that

$$\frac{dx}{dt} = \frac{\omega}{2}\frac{dx}{d\zeta} \qquad (2.21)$$

and

$$\frac{d^2x}{dt^2} = \frac{\omega}{2} \frac{d}{d\zeta} \left(\frac{\omega}{2} \frac{dx}{d\zeta}\right) = \frac{\omega^2}{4} \frac{d^2x}{d\zeta^2} \tag{2.22}$$

If Equation (2.22) is now substituted into Equation (2.17), the following equation of motion in the x direction results.

$$\frac{m\omega^2}{4} \frac{d^2x}{d\zeta^2} = - 2 Z e(U + V \cos 2 \zeta) \frac{x}{r_o^2} \tag{2.23}$$

or

$$\frac{d^2x}{d\zeta^2} = - \left[\frac{8ZeU}{m\omega^2 r_o^2} + \frac{8ZeV}{m\omega^2 r_o^2} \cos 2 \zeta\right] x \tag{2.24}$$

Now define the "variable" constants,

$$a = \pm \frac{8ZeU}{m\omega^2 r_o^2} \tag{2.25}$$

and

$$q = \pm \frac{4ZeV}{m\omega^2 r_o^2} \tag{2.26}$$

so that Equation (2.24) takes the following form.

$$\frac{d^2y}{d\zeta^2} + (a + 2 q \cos 2 \zeta) x = 0 \tag{2.27}$$

Beginning with Equation (2.18) and following the same procedure, the equation of motion for the y direction is obtained.

$$\frac{d^2y}{d\zeta^2} - (a + 2 q \cos 2 \zeta) y = 0 \tag{2.28}$$

The Equations (2.27) and (2.28) which describe the motion of

the charged particles in the electric field, given by Equation (2.12), are differential equations of the "Mathieu type." The behavior of the particles is thus governed by the properties of the solutions of these equations (McLachlan, 1964). The Mathieu equation is a linear, second order differential equation with constant, periodic coefficients. Either Equation (2.27) or (2.28) is considered to be in the normal form, if appropriate signs are assigned to the constants "a" and "q". This form was obtained by Mathieu, while solving for the vibrational modes of a stretched membrane with an elliptical boundary in 1868, and is given here by the following,

$$\frac{d^2 u}{d\psi^2} + (a - 2 q \cos 2\psi) u = 0 \qquad (2.29)$$

Negative values of "q", or a phase shift or $\pm \pi/2$ applied to Equation (2.29) yields the equation describing the motion of the charged particles in the x - direction. Negative values of "a" yield the equation of motion in the y - direction.

The general solution to Equation (2.29) is given,

$$u = A e^{\mu\psi} \sum_{-\infty}^{\infty} C_n e^{in\psi} + B e^{-\mu\psi} \sum_{-\infty}^{\infty} C_n e^{-in\psi} \qquad (2.30)$$

(u) is bounded for values of (μ) which are pure imaginary; otherwise (u) will increase exponentially. For imaginary values of (μ), the value of (u) will oscillate in some stable range, depending on the parameters, "a" and "q".

The ranges of stability for the solutions of the Mathieu equation are illustrated in Figure 1. From these curves, it is easily seen that the stability ranges are symmetric about q = 0. Now since
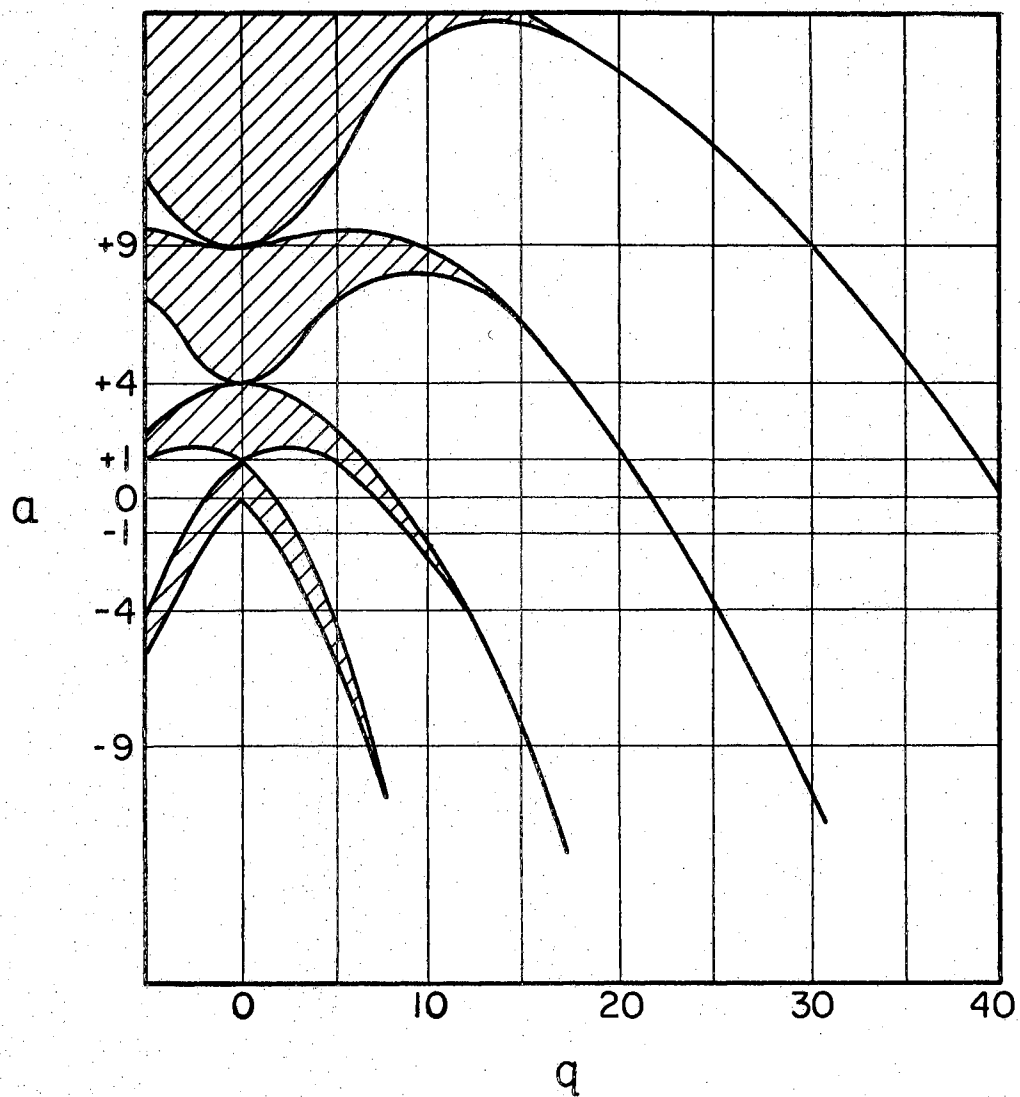
RANGES OF STABILITY FOR
SOLUTIONS OF MATHIEU EQUATIONS

Figure 1. Mathieu Stability Ranges

"a" must satisfy stability requirements in both the x and y direc-
tions, then the graph may be folded along the a = 0 axis.

A blown-up version of the first stability range, thus obtained,
is shown in Figure 2. As indicated on this graph, an operating
point of a = 0.2 and 2 = 0.7 has been chosen for the applications in
this work. This point yields an operating slope of a/q = 0.286,
which compares favorably with a typical operating slope of a/q = 0.310
used by the other experimenters in the field (Norgren and others,
1965).

It should be noted from Figure 2 that the operating point is
not at the apex of the stability region. Although to use the apex
as an operating point is desirable for some applications, such as
isotope scanning where extremely high resolution is demanded, the
resolution is quite sufficient at the point chosen for our purposes.

Attention should now be directed to the hyperbolic fields for
which the above solutions apply. The quadrupole mass filter, itself,
is not constructed of hyperbolic rods; rather, it is composed of
field electrodes which are hollow, cylindrical rods, which are spaced
and held in place according to the relation,

$$r = 1.15 \ r_o \qquad\qquad (2.31)$$

where: r = rod radius

r_o = quadrupole field radius

It can be shown that this relation is essential for hyperbolic
simulation, and is accurate to 1.0 percent.

The actual dimensions of the field rods will be dealt with in
the next chapter. The important point to be made here is that the
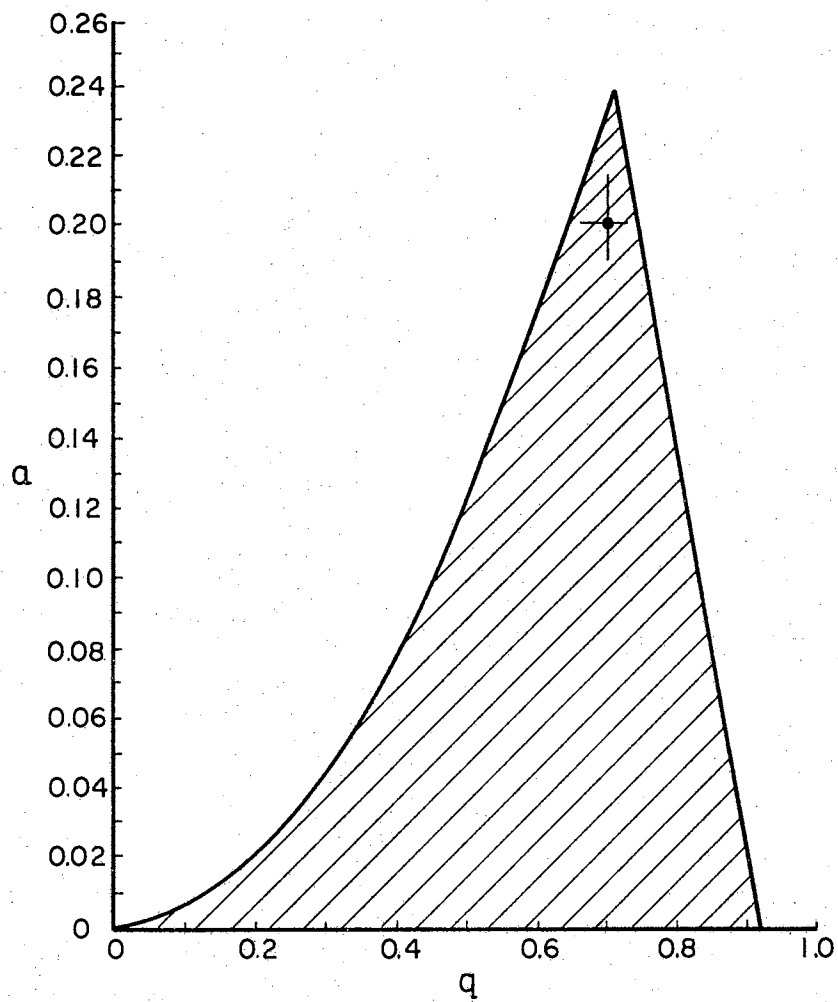
FIRST STABILITY RANGE
FOR MATHIEU SOLUTIONS

Figure 2. Mass Filter Operating Point

foregoing derivations are completely valid for cylindrical electrodes, so long as the relation (2.31) is observed. Figures 3 and 4 illustrate this hyperbolic simuluation.

Since the resolution is obviously increased, that is the field has a greater chance to eject unwanted q/m ratios, with the number of cycles an ion experiences in this field, the frequency of the driving rf voltage is a determining factor. It should be noted that the length of the electrodes is also involved in chosing the proper frequency, as is illustrated by the following considerations.

Noting that,

$$\omega t = n \, 2 \, \pi \tag{2.32}$$

where $\quad \omega = 2 \, \pi \, f \tag{2.33}$

and $\quad 1 = v_x t \tag{2.34}$

then $\quad n = f \, 1/v_x \tag{2.35}$

where $\quad \omega$ = angular driving frequency

$\quad 1$ = length of field; hence the length of the quadrupole electrodes

$\quad v_x$ = velocity of incident ions in the x - direction

$\quad n$ = number of cycles

With Equation (2.35) in mind, the procedure is then to choose a convenient field length (1) and then determine an upper limit on the velocity of incident ions. For our purposes, an electrode length of 30.0 cm was chosen. It was estimated from preliminary calculations that a maximum incident velocity of the order of 10^7 cm/sec could be used for this value for frequency determining purposes. It was found that an rf driving frequency of 3.2 X 10^6 cycles/sec would
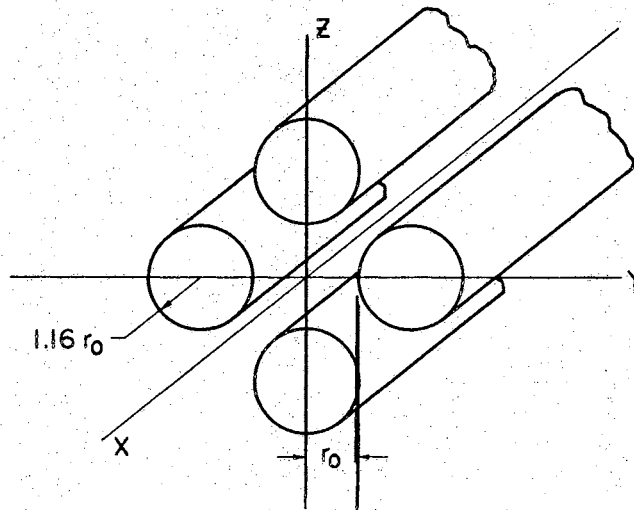
Figure 3. Actual Cylindrical Surfaces
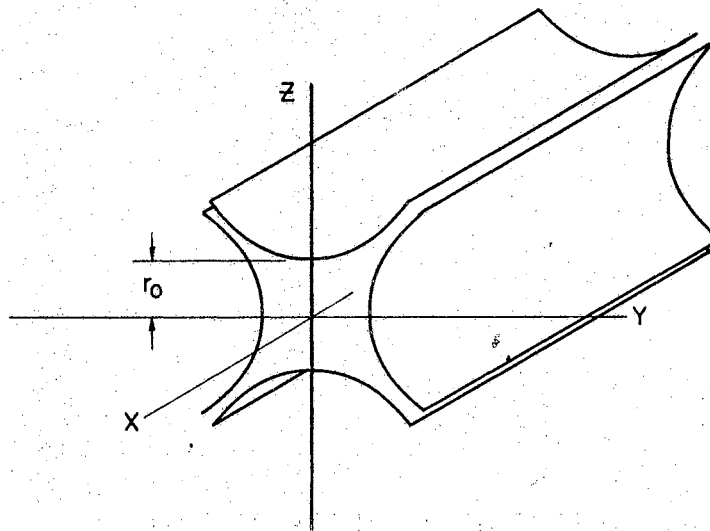
Figure 4. Ideal Hyperbolic Surfaces

cause the ions to experience 9.6 cycles while traversing the electrode field at a velocity of 10^7 cm/sec.

It can be readily seen from Equation (2.35) that ions of lesser incident velocity will experience proportionally more cycles in the field; hence the reason for the upper velocity limit.

The ion trajectories in the quadrupole field are very complicated and will not be gone into at this point. However, a graphic illustration, after Dawson and Whetten (1968), is presented in Figure 5. In this figure some ion trajectories are shown as the displacement of an ion from the center in one direction as a function of time. The upper trajectory shows an unbounded ion whose displacement grows in time. The center ion has a path which is oscillatory through the center, but whose amplitude continues to increase. The lower ion path is bounded, representing an ion that is contained in the field. The important point to note here is not the details of each trajectory, but the fact that the lower trajectory is stable in the field for the proper parameter settings. The parameter settings are referring to the proper dc and rf voltage which, in turn, are determined by the values of "a" and "q" as given by Equations (2.25) and (2.26).

Let us now consider these parameters as they affect the selection of a particular ion from a plasma which contains several specie. If we choose, for example, to monitor only those aluminum ions which are missing one electron, i.e., Al II or Al^{+1}, then the necessary voltages are calculated in the following manner.

Using Equation (2.25), the values which have been determined are substituted to solve for U, the dc voltage. Rewriting this
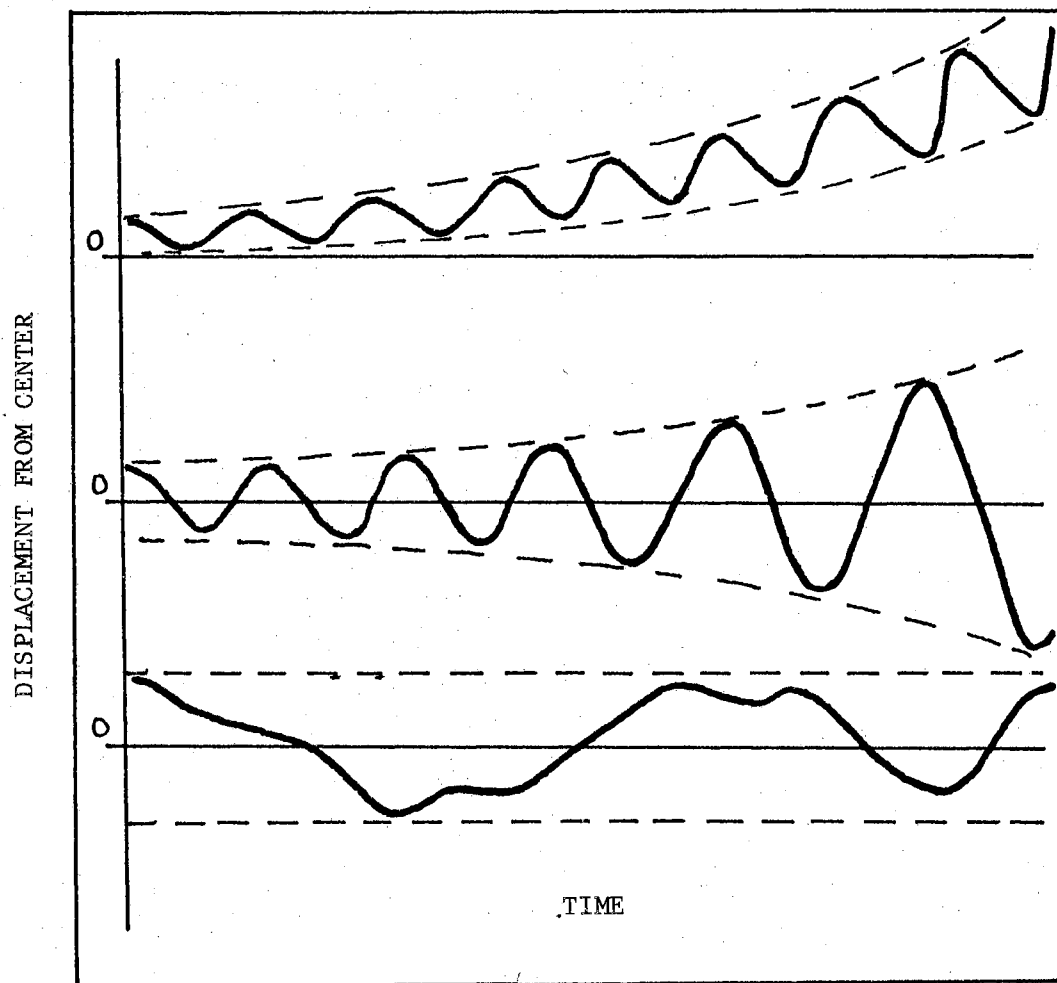
Figure 5. Quadrupole Ion Trajectories

equation yeilds,

$$U = \pm \frac{m\omega^2 r_o^2 a}{8Ze} \qquad (2.36)$$

Since Al^{+1} has been selected to be monitored, the degree of ionization, Z, assumes the value, $Z = 1$. (Al^{+1} is a singly-ionized aluminum atom.) The remaining variable values are summarized below.

$$\begin{aligned}
m &= 27 \text{ amu} = 4.48 \times 10^{-26} \text{ kg} \\
\omega^2 &= (2\pi f)^2 \\
f &= 3.2 \times 10^6 \text{ cycles/sec} \\
\omega^2 &= 4.04 \times 10^{14} \text{ (rad/sec)}^2 \\
r_o^2 &= 3.31 \times 10^{-5} \text{ (meters)}^2 \\
a &= 0.2 \\
q &= 0.7 \\
e &= 1.602 \times 10^{-19} \text{ Coulombs}
\end{aligned} \qquad (2.37)$$

The voltage is then given the following value,

$$U = 93.63 \text{ volts} \qquad (2.38)$$

This same procedure is followed using Equations (2.26) and (2.37) to arrive at the necessary value for the rf voltage, which is given as,

$$V = 655.4 \text{ volts} \qquad (2.39)$$

If it is assumed that the mass of the aluminum ion is constant, regardless of the ionization, i.e., neglect the electronic mass in favor of the nucleus, then for the entire range of possible ions, $1 \leq Z \leq 13$, the proper voltages are determined with the following

relations:

$$U = \frac{93.63}{Z} \quad \text{volts} \tag{2.40}$$

$$V = \frac{655.4}{Z} \quad \text{volts} \tag{2.41}$$

where the value of V is one-half the peak-to-peak amplitude of the rf voltage.

In the following tables are presented the dc and rf voltages for each ionic specie of aluminum up to Al^{+10}. In addition, the parameter values of "a" and "q" are given in each case to show the exclusion of all but one specie for a particular set of voltage values.

Notice that the accepted ion in each case corresponds to the values $a = 0.2$ and $q = 0.7$. If the values "a" and "q" for the rejected ions are compared with the stability region, given in Figure 2, it will be seen that the point corresponding to those coordinates lies outside the region.

TABLE I

STABILITY PARAMETERS FOR AL +1

$$Z \quad = \quad 1$$

$$U \quad = \quad \pm 93.63 \quad \text{volts}$$

$$V \quad = \quad \pm 655.4 \quad \text{volts}$$

Z	a	q	Classification
1	0.20	0.70	accepted
2	0.40	1.40	rejected
3	0.60	2.10	rejected
4	0.80	2.80	rejected
5	1.00	3.50	rejected
6	1.20	4.20	rejected
7	1.40	4.90	rejected
8	1.60	5.60	rejected
9	1.80	6.30	rejected
10	2.00	7.00	rejected
11	2.20	7.70	rejected
12	2.40	8.40	rejected
13	2.60	9.10	rejected

TABLE II

STABILITY PARAMETERS FOR AL +2

$$Z = 2$$

$$U = \pm 46.82 \text{ volts}$$

$$V = \pm 327.7 \text{ volts}$$

Z	a	q	Classification
1	0.10	0.35	rejected
2	0.20	0.70	accepted
3	0.30	1.05	rejected
4	0.40	1.40	rejected
5	0.50	1.75	rejected
6	0.60	2.10	rejected
7	0.70	2.45	rejected
8	0.80	2.80	rejected
9	0.90	3.15	rejected
10	1.00	3.50	rejected
11	1.10	3.85	rejected
12	1.20	4.20	rejected
13	1.30	4.55	rejected

TABLE III

STABILITY PARAMETERS FOR AL +3

$$Z = 3$$

$$U = \pm 31.21 \text{ volts}$$

$$V = \pm 218.5 \text{ volts}$$

Z	a	q	Classification
1	0.07	0.23	rejected
2	0.13	0.47	rejected
3	0.20	0.70	accepted
4	0.27	0.93	rejected
5	0.33	1.17	rejected
6	0.40	1.40	rejected
7	0.47	1.63	rejected
8	0.53	1.87	rejected
9	0.60	2.10	rejected
10	0.67	2.33	rejected
11	0.73	2.57	rejected
12	0.80	2.80	rejected
13	0.87	3.03	rejected

TABLE IV

STABILITY PARAMETERS FOR AL +4

$$Z = 4$$

$$U = \pm\ 23.41\ \text{volts}$$

$$V = \pm\ 163.85\ \text{volts}$$

Z	a	q	Classification
1	0.05	0.18	rejected
2	0.10	0.35	rejected
3	0.15	0.53	rejected
4	0.20	0.70	accepted
5	0.25	0.88	rejected
6	0.30	1.05	rejected
7	0.35	1.23	rejected
8	0.40	1.40	rejected
9	0.45	1.58	rejected
10	0.50	1.76	rejected
11	0.55	1.93	rejected
12	0.60	2.11	rejected
13	0.65	2.28	rejected

TABLE V

STABILITY PARAMETERS FOR AL +5

Z = 5

U = ± 18.73 volts

V = ± 131.1 volts

Z	a	q	Classification
1	0.04	0.14	rejected
2	0.08	0.28	rejected
3	0.12	0.42	rejected
4	0.16	0.56	rejected
5	0.20	0.70	accepted
6	0.24	0.84	rejected
7	0.28	0.98	rejected
8	0.32	1.12	rejected
9	0.36	1.26	rejected
10	0.40	1.40	rejected
11	0.44	1.54	rejected
12	0.48	1.68	rejected
13	0.52	1.82	rejected

TABLE VI

STABILITY PARAMETERS FOR AL +6

$$Z \quad = \quad 6$$

$$U \quad = \quad \pm \quad 15.61 \quad \text{volts}$$

$$V \quad = \quad \pm \quad 109.2 \quad \text{volts}$$

Z	a	q	Classification
1	0.03	0.12	rejected
2	0.07	0.23	rejected
3	0.10	0.35	rejected
4	0.13	0.47	rejected
5	0.17	0.59	rejected
6	0.20	0.70	accepted
7	0.23	0.82	rejected
8	0.27	0.94	rejected
9	0.30	1.05	rejected
10	0.33	1.17	rejected
11	0.37	1.29	rejected
12	0.40	1.40	rejected
13	0.43	1.52	rejected

TABLE VII

STABILITY PARAMETERS FOR AL +7

$$Z = 7$$

$$U = \pm 13.38 \text{ volts}$$

$$V = \pm 93.63 \text{ volts}$$

Z	a	q	Classification
1	0.03	0.10	rejected
2	0.06	0.20	rejected
3	0.09	0.30	rejected
4	0.11	0.40	rejected
5	0.14	0.50	rejected
6	0.17	0.60	rejected
7	0.20	0.70	accepted
8	0.23	0.80	rejected
9	0.26	0.90	rejected
10	0.29	1.00	rejected
11	0.31	1.10	rejected
12	0.34	1.20	rejected
13	0.37	1.30	rejected

TABLE VIII

STABILITY PARAMETERS FOR AL +8

$$Z = 8$$

$$U = \pm 11.70 \text{ volts}$$

$$V = \pm 81.92 \text{ volts}$$

Z	a	q	Classification
1	0.03	0.09	rejected
2	0.05	0.18	rejected
3	0.08	0.26	rejected
4	0.10	0.35	rejected
5	0.13	0.44	rejected
6	0.15	0.53	rejected
7	0.18	0.61	rejected
8	0.20	0.70	accepted
9	0.23	0.79	rejected
10	0.25	0.88	rejected
11	0.28	0.96	rejected
12	0.30	1.05	rejected
13	0.33	1.14	rejected

TABLE IX

STABILITY PARAMETERS FOR AL +9

$$Z = 9$$

$$U = \pm \ 10.40 \ \text{volts}$$

$$V = \pm \ 72.82 \ \text{volts}$$

Z	a	q	Classification
1	0.02	0.08	rejected
2	0.04	0.16	rejected
3	0.07	0.23	rejected
4	0.09	0.31	rejected
5	0.11	0.39	rejected
6	0.13	0.47	rejected
7	0.16	0.54	rejected
8	0.18	0.62	rejected
9	0.20	0.70	accepted
10	0.22	0.78	rejected
11	0.24	0.86	rejected
12	0.27	0.93	rejected
13	0.29	1.01	rejected

TABLE X

STABILITY PARAMETERS FOR AL +10

$$Z = 10$$

$$U = \pm 9.36 \text{ volts}$$

$$V = \pm 65.54 \text{ volts}$$

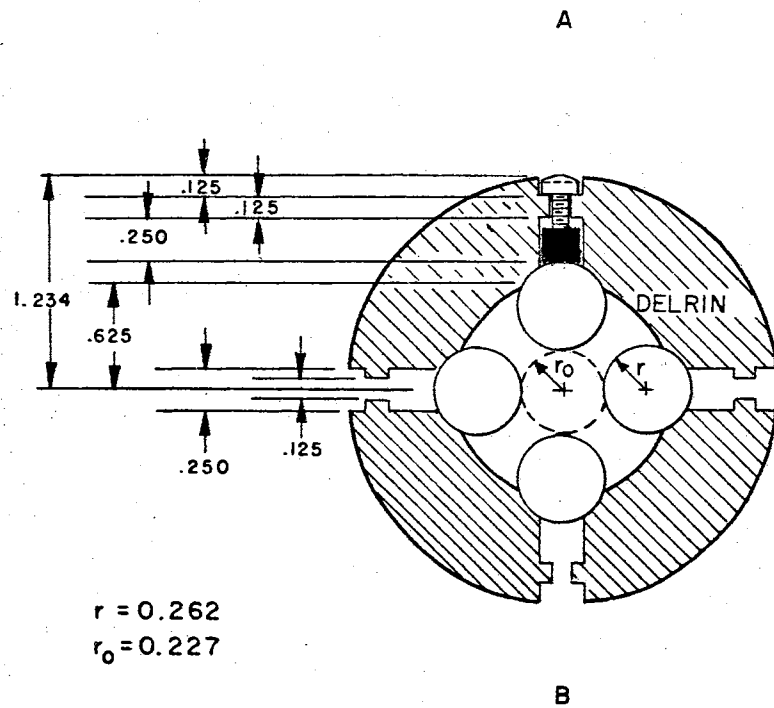| Z	a	q	Classification
1	0.02	0.07	rejected
2	0.04	0.14	rejected
3	0.06	0.21	rejected
4	0.08	0.28	rejected
5	0.10	0.35	rejected
6	0.12	0.42	rejected
7	0.14	0.49	rejected
8	0.16	0.56	rejected
9	0.18	0.63	rejected
10	0.20	0.70	accepted
11	0.22	0.77	rejected
12	0.24	0.84	rejected
13	0.26	0.91	rejected

CHAPTER III

QUADRUPOLE DESIGN AND CONSTRUCTION

Introduction

The quadrupole mass filter was designed to fulfill a specific need for analyzing the charged particles, which along with the neutrals, constitute the aluminum plasmas. The aluminum ions were of principle interest, so the discussion of the theory has been restricted to that pertaining only to the ions. The requirements for ion filtering (Peery, 1967) were determined and are presented below:

(1) A field length of 30 cm which requires four poles of diameter 13.23 mm and separation 11.50 mm.

(2) A radio frequency generator which operates at 3.2 mhz and which operates in the range from 0 to 1,000 volts peak to peak.

(3) A dc power supply which is variable from 0 to 150 volts. These requirements were basic to the design and each was met without difficulty. As was mentioned in Chapter II, the judicious spacing of the field rods or electrodes to maintain hyperbolic simulation yields the separation distance as given in (1) above. Figure 6 gives both a cross-sectional and a side view of the spacing arrangement. The nickel cylinders were obtained commercially and had an outside diameter of that given in (1) above. The spacer

33

CROSS SECTION VIEW   SIDE VIEW

A   A

DELRIN

.125
.125
.250
1.234
.625

r₀ r

r = 0.262
r₀ = 0.227

B

1.000
.125
.250
1.234
NICKEL
FIELD ROD

DELRIN
SPACER

.250
.500
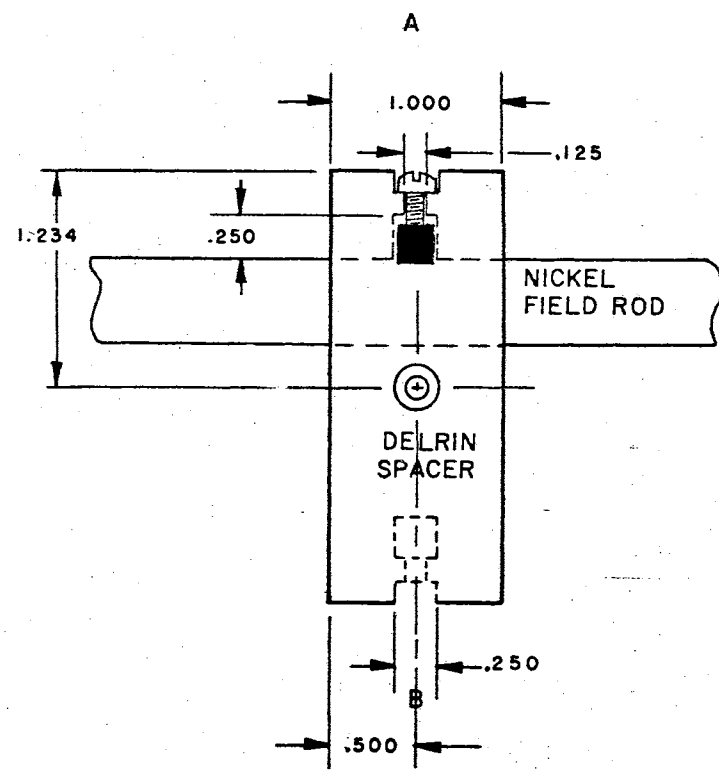
1 inch
full scale

Figure 6.   Quadrupole Field Electrode Spacers

34

is constructed of Delrin which was machined to hold the rods at the

proper separation distances. Two such spacers were constructed and

the cylinders were attached as shown in Figure 6. A calibration rod

was carefully machined to a diameter of 11.50 mm and was used to hold

the cylinders in place while the containing screws holding them to

the spacers were adjusted. After the screws were tightened into

place, the calibration rod was then removed, leaving the field radius

at the proper value. The nickel cylinders, held in place by the

Delrin spacers, then constitute the quadrupole lens system.

Quadrupole Power Supply

The power supply providing the high rf voltage was constructed

according to the schematic shown in Figure 7. Included in the

power supply is a power transformer which steps wall voltage up to

3 KV, which is then rectified using two mercury vapor diode tubes

(866-A). The output is then fed to a class "C" oscillator circuit,

which employes two oscillator tubes (4-65 A) and which provides

0 - 3000 VAC at 3.2 MHz. The same transformer provides 0 - 300 VDC,

plus and minus, for superposition on the quadrupole electrodes. A

large air condenser provides several continuously variable frequency

settings, with 3.2 MHz at about mid-range. As will be noticed above,

the design requirements for the power supply were exceeded so that

a versatile piece of equipment was produced which may be used with

the quadrupole lens to investigate elements other than aluminum.

For all of the investigations done with the quadrupole mass filter,

the frequency was maintained constant at 3.2 MHz. The maximum rf

voltage required obtained for the Al^{+1} specie of aluminum and had

Figure 7. Schematic of Quadrupole Power Supply

the value 1310.8 volts peak-to-peak. The maximum dc voltage require-
ment for aluminum ions occurred for the Al^{+1} specie also, and had
the value 93.63 volts. As an indication of low voltage requirements,
for the specie Al XI, the values are given, respectively, 65.54 VAC
peak-to-peak and 9.46 VDC.

In Figure 8 will be seen the diagram of the power supply as it
was used to provide the necessary voltages on the quadrupole field
electrodes.

Quadrupole Vacuum System

The vacuum system for the quadrupole mass filter consists essen-
tially of a nickel plated cylinder of 4.0 in inside diameter and
15.0 inches in length. This vacuum envelope has a flange opening
at a point half way between the two ends, onto which is bolted a
diffusion pump. At one end of the envelope is a one and three-fourths
inch opening which provides an entrance to the glass manifold. At
the other end of the envelope is attached a 7.0 inch spacer which
was constructed to allow enough room inside the vacuum system for
the electron multiplier. This causes the over-all length of the
envelope to be in the neighborhood of 22.0 inches. At the end of
this spacer is bolted a flange plate to close the system. Electrical
feedthroughs built into this flange plate permit the transmission of
power to the quadrupole electrodes and electron multiplier inside
the vacuum system, as well as the transmission of the multiplier out-
put signal to the 585 Tektronic oscilloscope. A diagram of the
quadrupole assembly inside the vacuum envelope is given in Figure 9.

The diffusion pump was obtained from the Consolidated Vacuum

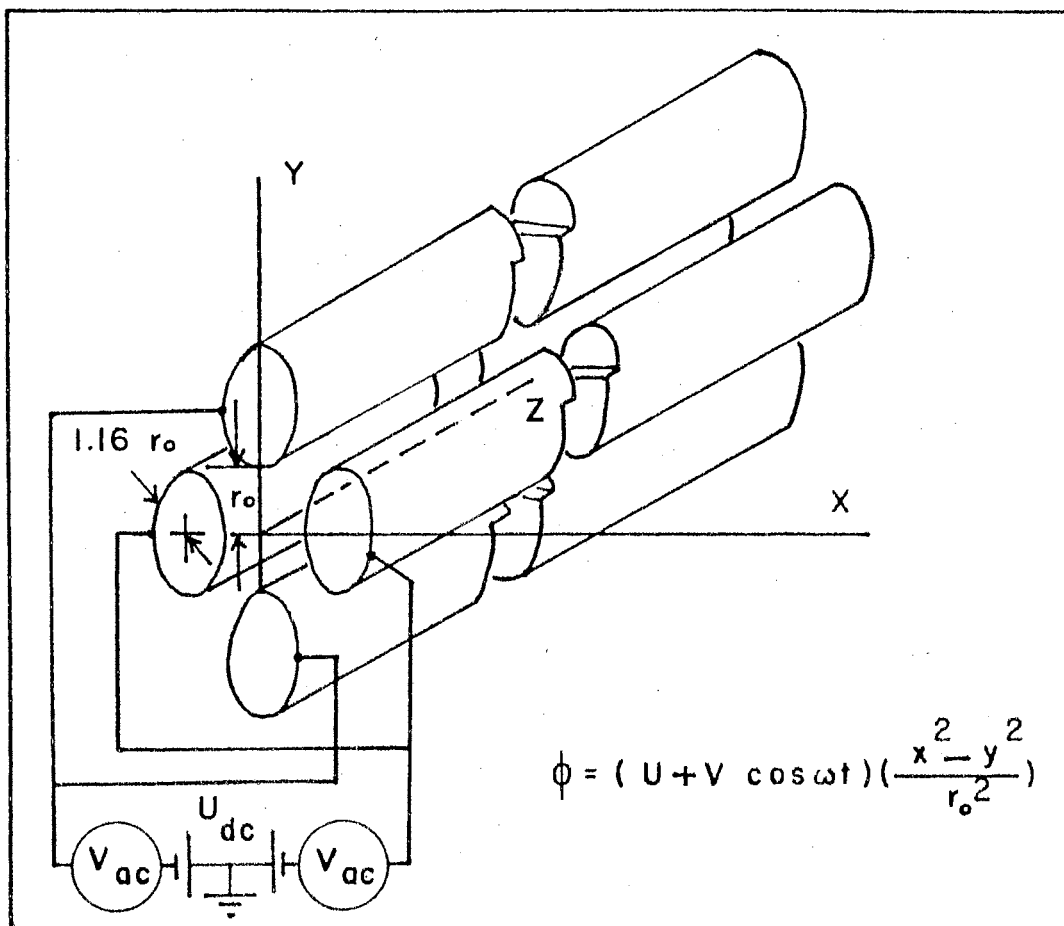$$\phi = (U + V \cos \omega t)(\frac{x^2 - y^2}{r_o^2})$$
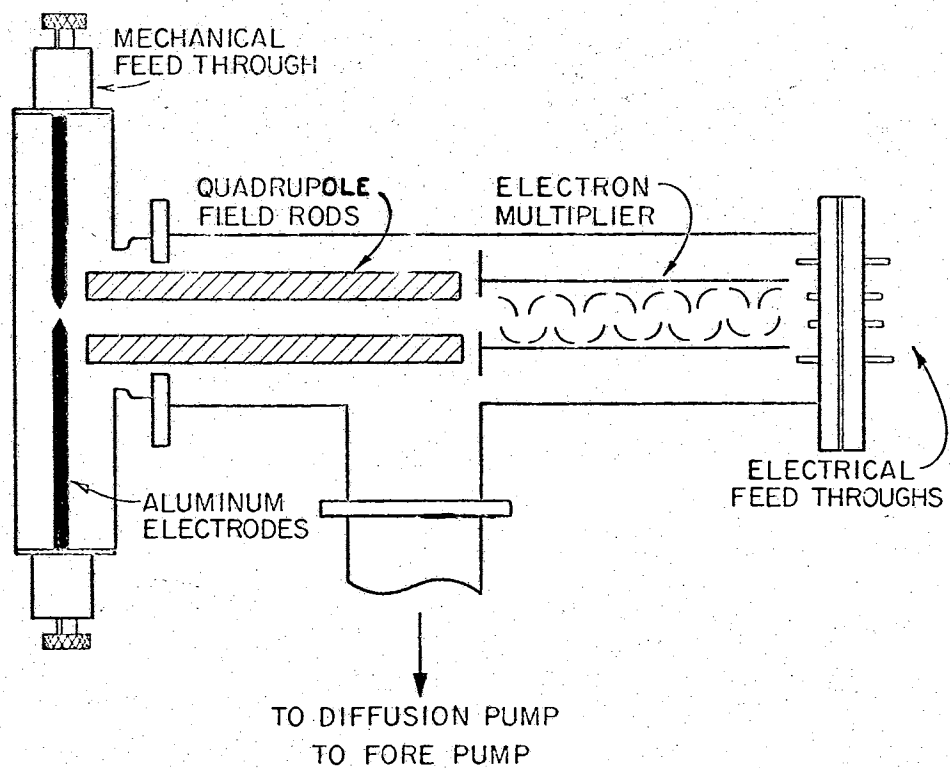
Figure 8. Diagram of Quadrupole Electrode Arrangement

Figure 9. Quadrupole Assembly in Vacuum

Corporation and is properly described as a fractionating oil diffusion pump, type MCF-300. This type requires 225 cc of vacuum pump fluid to operate and the type used was Convoil-20. It contains an external heater rated at 750 watts and is conveniently operated at line voltage. Cooling is provided by water coils through which the flow rate should be adjusted to 0.20 gallons per minute. One nice feature of this pump is that it may be turned on as soon as the fore pump pressure reaches a value of 500 microns or lower. This allows a faster evacuating rate, without the problem of contaminating the system with oil. It should be noted, however, that a baffle was constructed and placed between the envelope and the diffusion pump as an added precaution. The mechanical fore pump used with this system was a Duo Seal, type 1402, obtained from the Welch Scientific Company. The pressure of the system was monitored using two methods. A CVC thermocouple gauge tube, GTC-004, was used to measure pressure from atmospheric down to 1.0 micron. An ion tube, GIC-015-2, was used to measure pressures of 1.0 microns and lower. The output of both of these was taken from a CVC Ionization Gauge, type GIC-100.

Electron Multiplier

The detector system, mentioned before in the text, consist of an uncased, twenty stage copper-beryllium multiplier and the 585 Tektronic oscilloscope. The stages or Dynodes of the multiplier act as secondary electron emitters, as well as electron accelerators. The gain of this device depends on several factors, among which include the pressure and the accelerating voltage between successive dynodes. For the investigations completed with the quadrupole system,

voltages of the order of from 800-1000 volts were used from the

0-2.5KV power supply. With a voltage of 1000 volts supplied to the

multiplier, the gain may be conservatively given as 1.0 million. The

ions from the plasma source strike the first dynode, i.e., the cath-

ode. Electrons are emitted from the surface of this dynode via

secondary emission and are accelerated to the second dynode whereupon

more electrons are emitted. This process continues until the sec-

ondary electron current, which is the output of the last dynode, or

anode, is fed across a load resistor to the oscilloscope. No de-

tailed discussion on the electron multiplier will be given here since

the literature (Allen, 1939) available contains literally volumes on

the subject. A schematic diagram of the type of multiplier used by

this student is presented in Figure 10.

Data Collection

The 585 oscilloscope is used with a Tektronic type 86 plugin

unit which has high gain and a rise time of the order of 4.0 nano-

seconds. This instrument provides fixed deflection factors from

0.01 volts per centimeter to 50.0 volts per centimeter. Also a

variable sweep speed of from 2.0 seconds per centimeter to 50.0 nano-

seconds per centimeter are provided. The additional features of

single sweep and delayed sweep capability were invaluable to our data

collection techniques.

A Tektronic type C-12 camera was used to take pictures of the

oscilloscope traces for permanent records. Two types of film were

used for our purposes. Both are commercially available from Polaroid

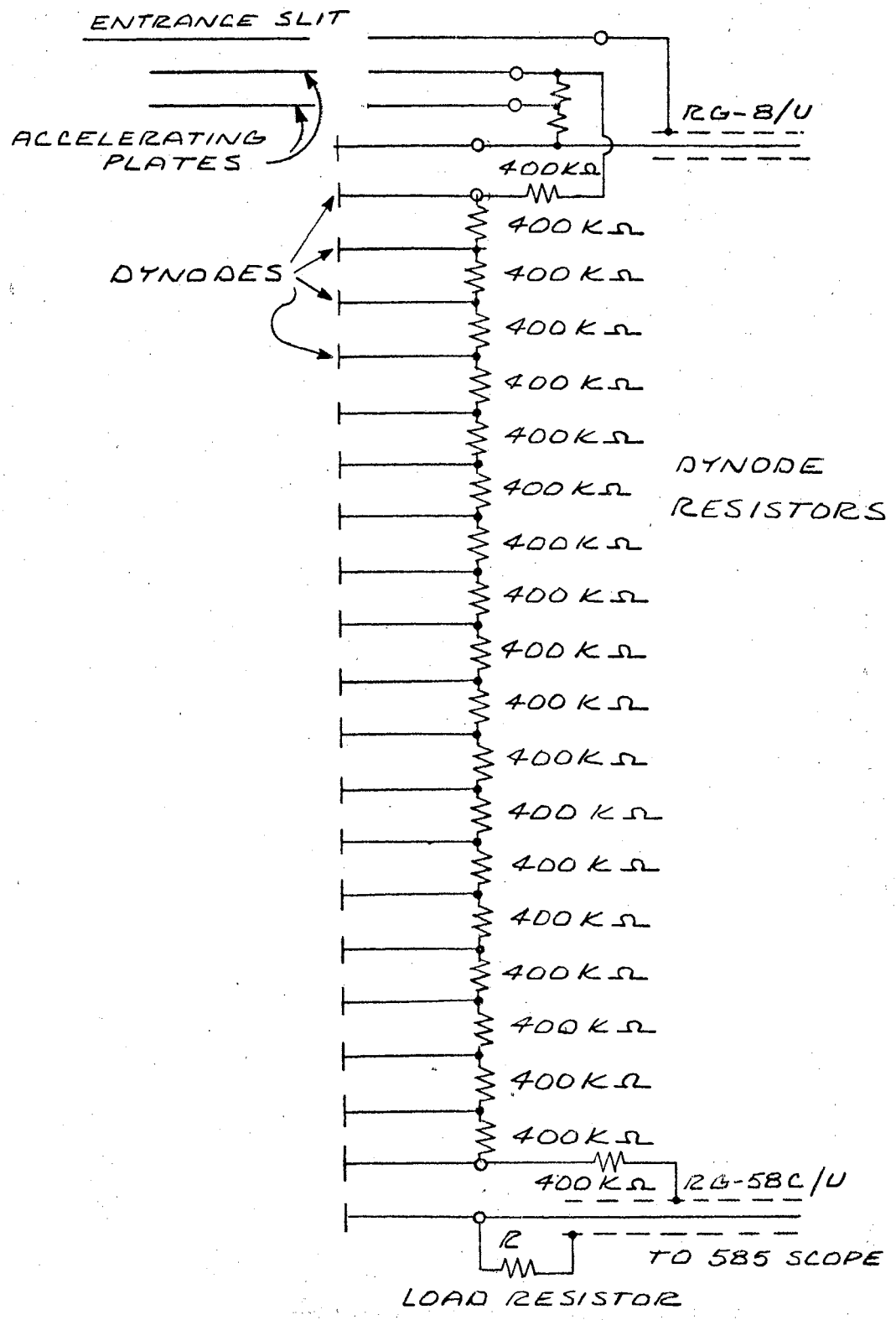and are given as type 47, 3000 ASA, and type 410, 10,000 ASA. The

Figure 10. Schematic of Electron Multiplier

later type of film was found to be especially well suited to the rapid

scan speeds used to monitor the initial bursts of ions, as well as

the earlier light pulse from both the breakdown of the spark elec-

trodes and the laser impact on aluminum. These photographs are then

enlarged for study and several of the curves taken directly from

these are presented in Chapter V.

In Figure 11 is presented a block diagram of the quadrupole

assembly in the operational mode for analyzing the spark discharge.

The high voltage power supply in the upper left of the diagram is

used to charge a General Electric pyranol capacitor, which is rated

at 1.0 microfarads and 12.5 kilovolts. This capacitor is then dis-

charged across the aluminum electrodes, producing the plasma to be

analyzed. The mechanical feedthroughs are used to vary the spark

gap separation. The optimum gap width was found to be of the order

of 1.0 mm. The power supply in the upper center-left provides the

accelerating voltage for the electron multiplier. This is a positive

ground power supply and is rated at from 0-2.5 kilovolts. The power

supply at the upper center-right provides the rf and dc voltages for

the quadrupole field electrodes. The oscilloscope in the upper right

monitors the magnitude of the rf voltage, the dc voltage and the

frequency of the rf voltage. Although this power supply has been

calibrated, the scope allows a constant check to insure that the

proper values are maintained throughout the data-collecting process.

The oscilloscope in the lower right of the figure monitors the out-

put of the electron multiplier. The C-12 camera is attached to this

scope.

A photograph of the quadrupole assembly is presented in Figure
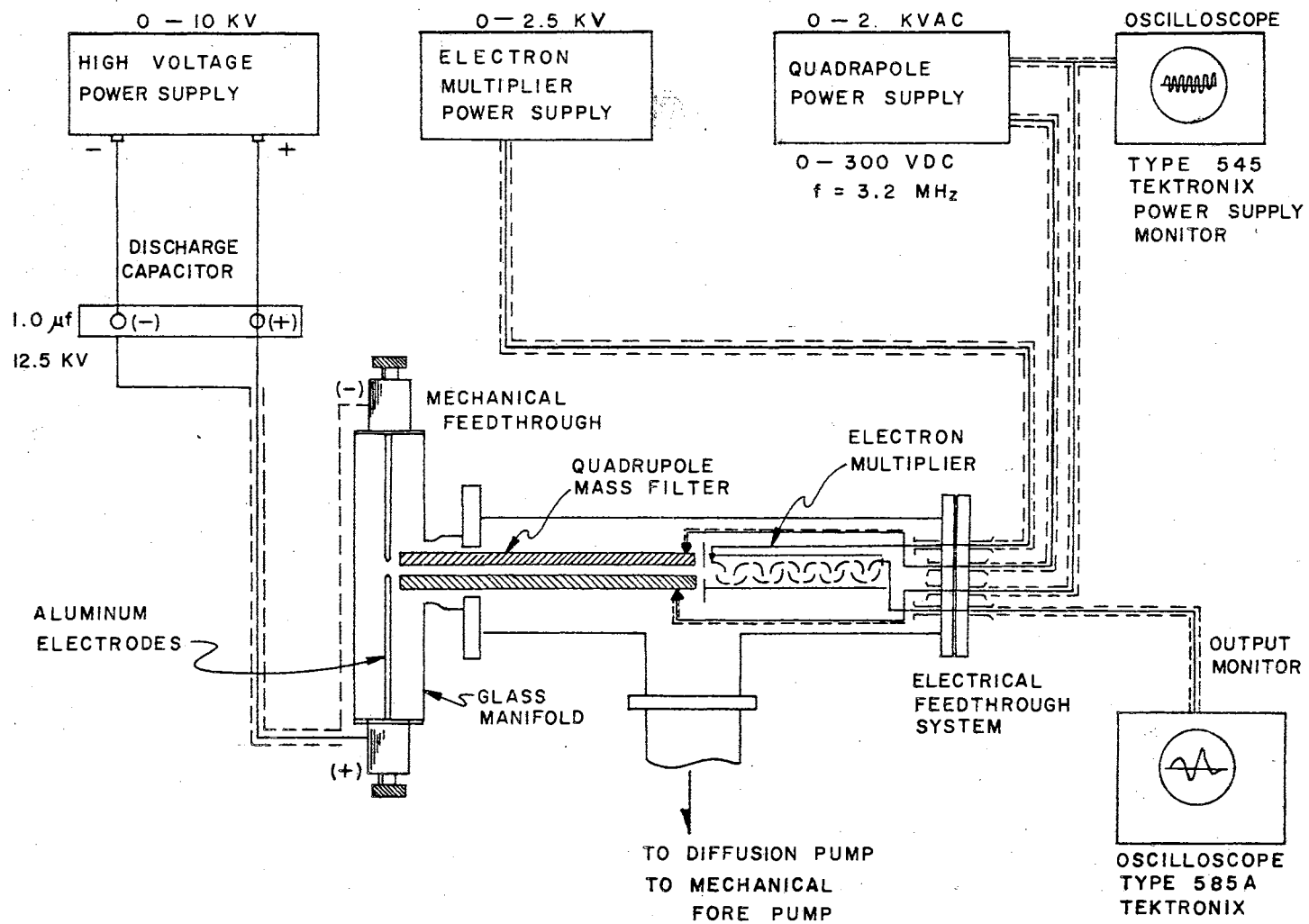
Figure 11. Block Diagram of Quadrupole Mass Filter and Support Equipment

12. This photograph shows the vacuum system, the vertical glass mani-
fold which contains the spectroscopically pure aluminum electrodes
and some of the support equipment necessary for operation. Figure 13
provides a picture of the quadrupole field electrodes in a glass in-
sulator sleeve. Also shown in this photograph, immediately to the
right of the field electrodes, is the uncased electron multiplier.
The flange plate with electrical feedthroughs are shown at the ex-
treme right. At the extreme left will be seen two typical aluminum
spark electrodes which are tapered to a point. The device attached
to the front of the field electrodes is a pulsed electrostatic lens,
which will be discussed in Chapter IV. It should be noted that for
all the investigations reported in Chapter V, this device was not
inserted between the plasma source and the mass filter.

Figure 12. Photograph of the Quadrupole Assembly
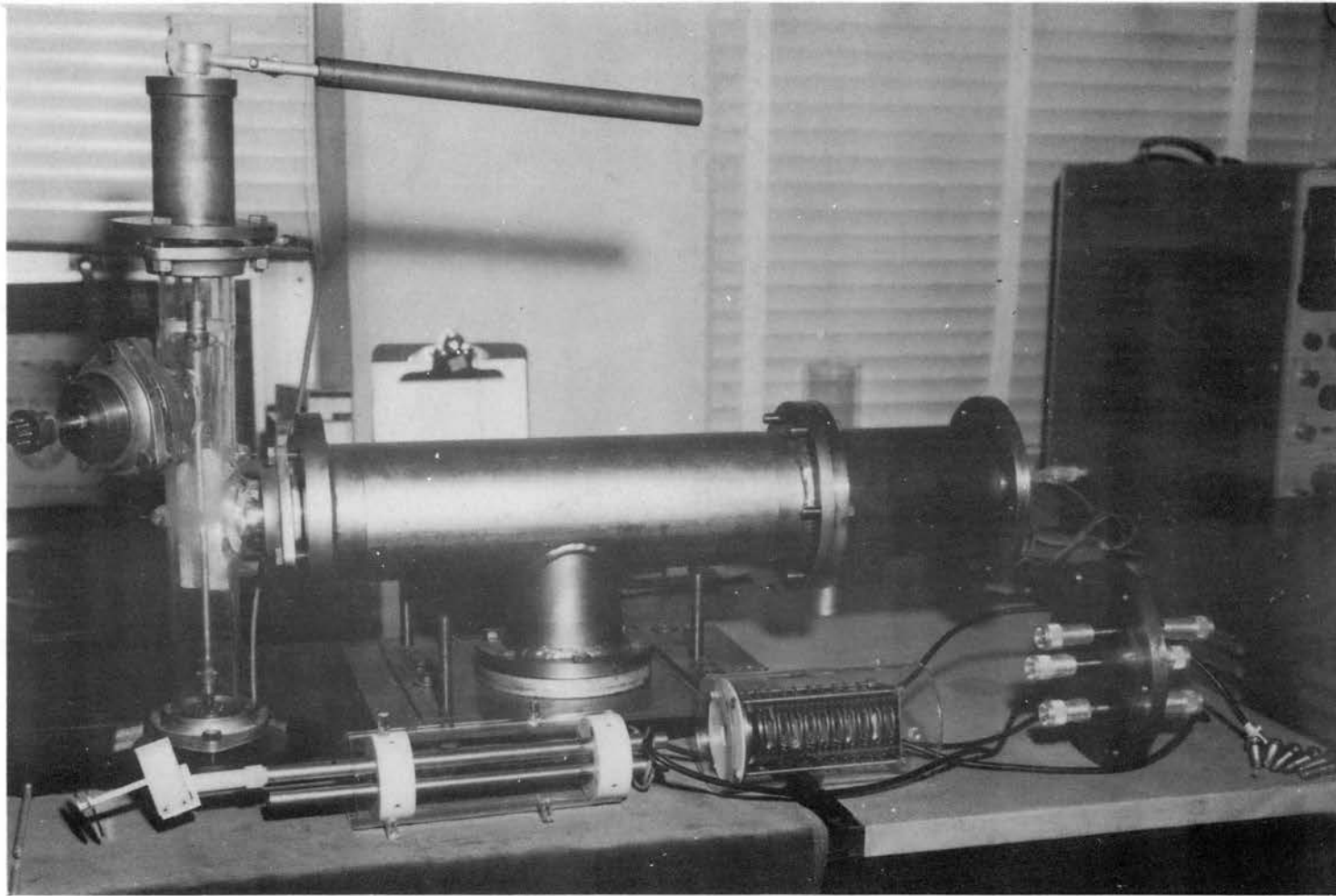
Figure 13. Quadrupole Field Electrodes and the Electron Multiplier

CHAPTER IV

THE PULSED ELECTROSTATIC LENS

Background Discussion

The work associated with analyzing beams of charged particles
has nearly always been involved, in some way, with the focusing or
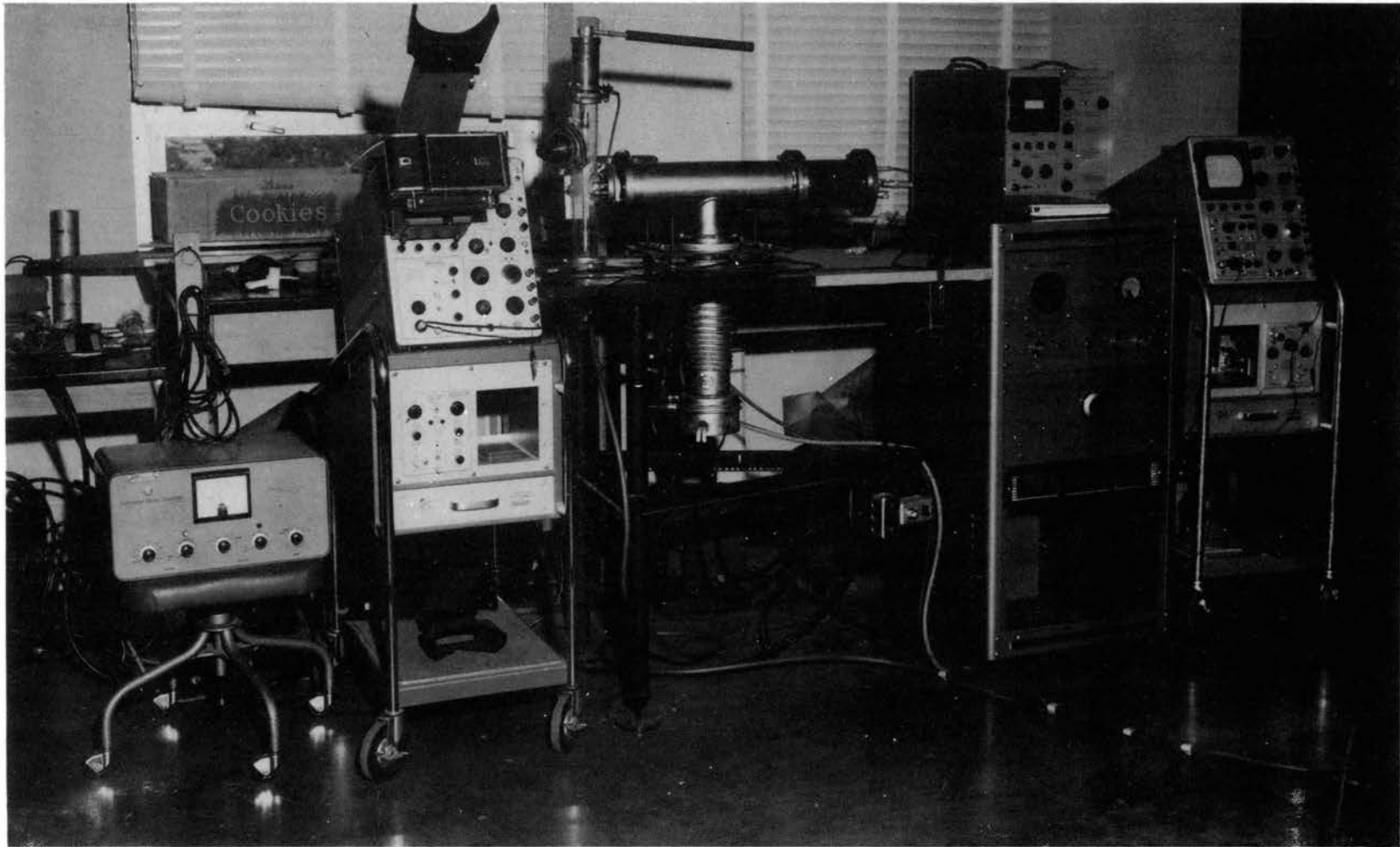collimating of such beams. In many instances, a combination of
electric and magnetic fields has been employed for this purpose,
depending on the particular requirements. In the case of magnetic
mass spectrometers, a magnetic field is necessary to alter the
trajectories of charge particles so that they may be identified. In
the study of elementary particles, huge magnets are used to contain
the particles as they are accelerated to great velocities. It will
be remembered that in the Millikan oil drop experiment of 1917,
parallel plates were employed to create an electric field to counter
the gravitational force on the charged oil drops. Then from pith
balls to electronic tubes to synchrocyclotrons, the use of electro-
magnetic fields to control the trajectories of charged particles is
well known.

It has already been discussed in Chapter II how alternating
electric fields are employed in the mass filter to control the tra-
jectories of aluminum ions as they traverse the quadrupole field.
The need for additional control over the ions to be monitored will
immediately be seen upon further investigation of the procedure of

48

plasma ion analysis.

Consider this simplified process of plasma production and emission. In the case of spark gap breakdown, energy is supplied to the plasma at the time of breakdown for approximately the duration of the capacitor discharge, thereby ionizing the vaporized atoms, as well as energizing the neutral atoms to a metastable state. Immediately thereafter, many of these metastable atoms undergo downward transitions in which light is produced. The resulting emission of the plasma which enters the quadrupole mass filter then consists, not only of ions, but of light and metastable atoms. The filtering action of the quadrupole will eliminate the undesired ionic species, but the light and uncharged metastable atoms pass through the filter undeflected. The light emission in the ultraviolet region and the metastable atoms which strike the first dynode of the electron multiplier, produce secondary electrons, just as do the ions.

The difficulty in reducing the data, as regards a quantitative measurement of relative ionic density and of ionic velocity distributions, can be recognized when the fact, that the light and metastable atoms are superposed on the output, is considered. It was precisely this fact that led to the initiation of the electrostatic lens system.

The desire to remove the neutral atoms and light from the ion beam, prompted the conception of several types of electric and/or magnetic fields to use for this purpose. The disadvantage of some of these lies in their distortion of the velocity distribution, as well as in their inability to handle several ionic specie in sucession. A variety of electrode geometries and voltage values were

considered and the final design is presented later in the test.

It was decided to eliminate the use of magnetic fields entirely and to design a device which could be used to focus all of the ions along a direction with as wide an angular separation from the light and neturals as practical. Since as in the quadrupole itself, the light and neutrals are unaffected by electric fields, they are allowed to pass through the lens along a straight line from the plasma source, while the ion trajectories are curved to the extent of the magnitude of the applied voltage to the lens electrodes.

Design and Construction

One of the fundamental requirements, considered in the design of the lens, was that all ions considered, regardless of their velocity, exit the lens at very closely the same angle and along the same direction. Of course, the ions enter the lens from the plasma source along with the light and neutrals. A simple parallel plate design was taken as a starting guide, but it was quickly seen that because of the velocity range of from 700 to 7000 meters per second of the ions, the angular exit spread was impossible to cope with. This was, of course, due to the ions, although of the same charge, spending different times in the uniform electric field of definite length. In order to overcome this difficult, a non-uniform field, resulting from an asymmetrical electrode geometry, was found to be suitable in theory, but the foreseen difficulty with construction of the electrodes and the problem of fringing discouraged this design.

A return to the basic parallel plate was the answer to our design questions. The key to the solution was to construct a solid

base plate, but to substitute discrete wire electrodes for the oppos-
ing plate. The obvious advantage in this arrangement is that a
different voltage may be placed on each of the wire electrodes, there-
by producing the desired electric field gradient necessary to focus
the ions, regardless of their velocities.

Figure 14 shows the field electrode wires and the base ground
plate as they are held in place by the Delrin insulator. It was
found that if the electric field of the electrostatic lens was
applied for 1.0 microseconds, the 7000 meter per second ions would
travel a distance of 7.0 mm in this time interval. Since the slower
ions will travel distances, proportionally shorter than this, the
effective field length of the lens was designed to be approximately
8.5 mm. It will be seen in Figure 14 that there are eleven field
electrodes. Only the central five of these electrodes provide the
critical electric field gradient. Three electrodes on either side
of these central five were inserted to provide a means to maintain
a fairly uniform, i.e., parallel, field in the central effective
region of the lens. This seems to be the solution to the fringing
problem. The potential on the first three electrodes is maintained
at the same potential as that on the first effective electrode. The
potential on the last three electrodes, which are closer to the exit
of the lens, is maintained at the same potential as that on the fifth
or last effective electrode. The base plate is always maintained at
ground potential.

The name, pulsed electrostatic lens, derives from the fact that
the effective field is acting only for a very short interval of time,
which in this case is 1.0 microsecond. This of course demands that

TO POWER SUPPLY

NICKEL WIRE
0.5mm

NICKEL
GROUND
PLATE

4.0 cm

0.62 in

2.0cm

DELRIN HOUSING

2.0 in
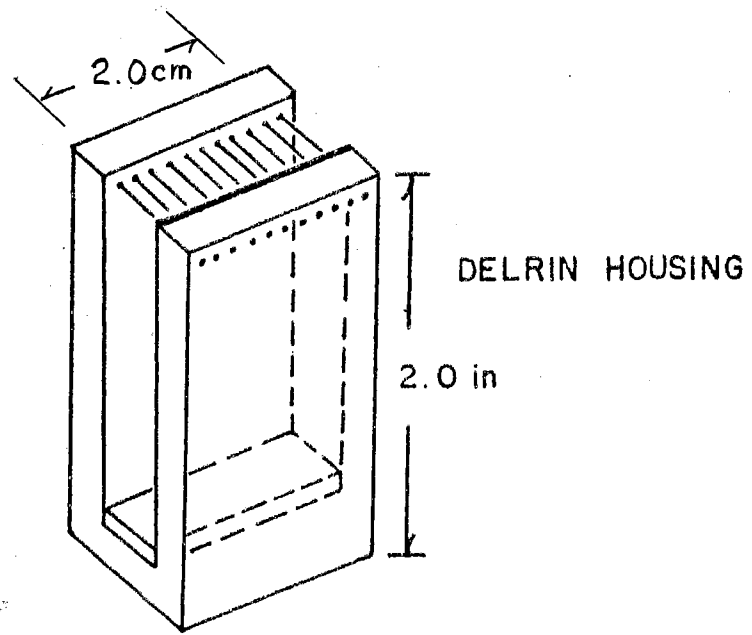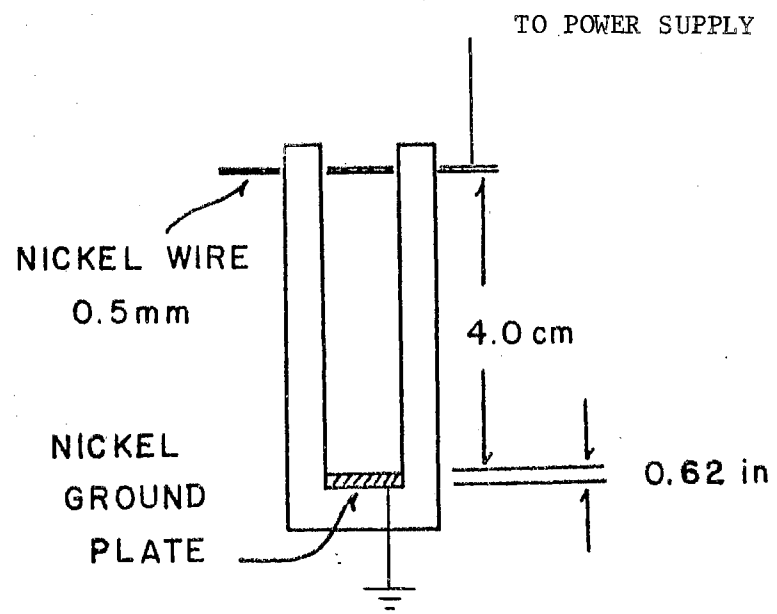
Figure 14.   Electrostatic Lens

the applied field be synchronized with the entry of the ions into the
lens.

<div align="center">Electrostatic Lens Theory</div>

Consider the emission of ions from a plasma which is then
directed into the region of an electric field, produced by the elec-
trostatic lens. The construction of the lens with spaced electrodes
necessitates the use of two equations of motion since the ions
directly above a wire electrode are in the region of a constant
electric field, whereas an ion between two electrodes is in the re-
gion of a space dependent field.

From Coulomb's law and Newton's second law the basic equation
of motion is determined:

$$\vec{F} = n\ e\ \vec{E} \tag{4.1}$$

$$\vec{F} = m\ \vec{a} \tag{4.2}$$

where: n = degree of ionization

Then the equation becomes:

$$m\ \vec{a} = n\ e\ \vec{E} \tag{4.3}$$

or

$$\frac{d^2\vec{y}}{d^2t} = \ddot{\vec{y}} = \frac{n\ e\ \vec{E}}{m} \tag{4.4}$$

Now since the electric field is given:

$$\vec{E} = E_y\ \vec{j} \tag{4.5}$$

one is concerned only with the vertical displacement of the ion in

the field. The velocity in the x-direction, i.e., the initial direction of ion travel, is unaltered by the field.

Then for an on-axis entry of the ions, i.e., with no initial vertical displacement, the equation of motion is then the solution to Equation (4.4).

Solving for the vertical displacement (y) in Equation (4.4),

$$\frac{dy}{dt} = \dot{y} = \frac{ne}{m} \int_o^t E \ dt \tag{4.6}$$

$$= \frac{ne}{m} Et + \left(\frac{dy}{dt}\right)_o$$

where: $E = \frac{V}{d}$ = constant

   V = accelerating potential

   d = vertical field separation

then:

$$y = \frac{ne}{m} E \int_o^t t \ dt + \int_o^t \left(\frac{dy}{dt}\right)_o \ dt \tag{4.7}$$

or

$$y = \frac{ne}{m} E \frac{t^2}{2} + \left(\frac{dy}{dt}\right)_o t + y_o \tag{4.8}$$

is given as a function of time in terms of the electric field (E), the degree of ionization (n), the electronic charge (e), the ionic mass (m), the initial vertical velocity $((dy/dt)_o)$ and the initial vertical displacement (y_o).

Through an obvious change of variables,

$$v = \frac{(x - x_o)}{t} \tag{4.9}$$

where: $v =$ velocity in x-direction

Equation (4.8) becomes:

$$y = \frac{n\ e\ E}{2\ m}\ (\frac{x - x_o}{v})^2 + \overset{o}{y_o}\ \frac{(x - x_o)}{v} + y_o \qquad (4.10)$$

where: $\overset{o}{y_o} = (\frac{dy}{dt})_o$

Now with the equation in this form, the slope of the ion trajectory is determined for any horizontal displacement. This slope is given:

$$\frac{dy}{dx} = \frac{n\ e\ E}{2\ m}\ \frac{2(x - x_o)}{v^2} + \frac{\overset{o}{y_o}}{v} \qquad (4.11)$$

The Equations (4.10) and (4.11) give the vertical displacement and slope of the ion trajectory for any horizontal displacement into the electric field. It is desirable to know the slope of the trajectory in terms of angular degrees above the horizontal or initial direction travel. This is given by the familiar form:

$$\text{TAN } \theta = \frac{dy}{dx}$$

or

$$\theta = \text{ARC TAN } \frac{dy}{dx} \qquad (4.12)$$

Therefore from Equation (4.11) the following expression for the slope is obtained:

$$\theta = \text{ARC TAN } [\frac{n\ e\ E}{2\ m}\ \frac{2(x - x_o)}{v^2} + \frac{\overset{o}{y_o}}{v}] \qquad (4.13)$$

The equations derived above are for a charged particle in the

parallel plate capacitor. They hold for the period in which the ions are directly above the electrode wires of the lens system.

In traversing the entire lens, the ions intermittently pass through regions between electrodes where the electric field is not constant, but an increasing function of $(\dot{x})$. The equation of motion for the ions in this region differ from those derived above to the extent that $E = E(x)$.

i.e.,
$$\ddot{y}(t) = \frac{n\ e\ E(x)}{m} = \frac{n\ e\ V\ (x)}{md} \tag{4.14}$$

where:
$$V(x) = V_o + \alpha\ x \tag{4.15}$$

and:
$$\alpha = \frac{\partial V}{\partial x} \ ,$$

the special increase of the potential in the direction of ion travel.

Solving for (y) in Equation (4.14), the equation of motion is obtained:

$$\dot{y}(t) = \frac{ne}{md} \int_o^t (V_o + \alpha\ x)\ dt \tag{4.16}$$

$$= \frac{ne}{md} \int_o^t (V_o + \alpha\ v\ t)\ dt$$

so that:

$$\dot{y}(t) = \frac{ne}{md} \left[V_o\ t + \frac{\alpha\ v\ t^2}{2}\right] + \dot{y}_o \tag{4.17}$$

and

$$y(t) = \frac{ne}{md} \int_o^t (V_o\ t + \frac{\alpha\ v\ t^2}{2})\ dt + \int_o^t \dot{y}_o\ dt \tag{4.18}$$

or

$$y(t) = \frac{ne}{md} \left[\frac{V_o \, t^2}{2} + \frac{\alpha \, v \, t^3}{6} \right] + \overset{\circ}{y}_o \, t + y_o \qquad (4.19)$$

With a change in variables, the equation of motion yields the vertical displacement as a function of (x) for the space dependent region of the electric field.

$$y(x) = \frac{ne}{md} \left[\frac{V_o \, (x - x_o)^2}{2 \, v^2} + \frac{\alpha (x - x_o)^3}{6 \, v^2} \right]$$

$$+ \frac{\overset{\circ}{y}_o \, (x - x_o)}{v} + y_o \qquad (4.20)$$

The slope is then given, similar to Equation (4.11) by the following:

$$\frac{dy \, (x)}{dx} = \frac{ne}{md} \left[\frac{V_o \, (x - x_o)}{v^2} + \frac{\alpha (x - x_o)^2}{2 \, v^2} \right] + \frac{\overset{\circ}{y}_o}{v} \qquad (4.21)$$

or

$$\theta = ARC \ TAN \left[\frac{ne}{md} \left[\frac{V_o \, (x - x_o)}{v^2} + \frac{\alpha (x - x_o)^2}{2 \, v^2} \right] \right.$$

$$\left. + \frac{\overset{\circ}{y}_o}{v} \right] \qquad (4.22)$$

Thus the ion trajectories are specified at any point through the lens system by Equations (4.10) and (4.12) over an electrode region and by Equations (4.20) and (4.22) over a space region.

Slopes of the Ion Trajectories

The equations derived above were used to predict the motion of

any ion, regardless of its charge or entrance velocity. The mass of
of the ions was taken as that of aluminum.

In the velocity range from 700 m/sec to 7000 m/sec the final
vertical deflection and slope of each ion specie has been calculated.
The minimum vertical deflection for the 1000 m/sec ion has the value
of 0.1171 mm and the maximum deflection occurs for the 7000 m/sec
ion and has the value of 0.5948 mm.

A computer program was used to calculate the optimum voltages
required to maintain a constant 15.00 degree slope. Using this value
of the slope as optimum, the following deviations were calculated.

The maximum value for the slope occurred for the 2500 m/sec
ion and is given: 17.13 degrees

The minimum value for the slope occurred for the 3500 m/sec
ion and is given: 12.64 degrees

The deviation from the optimum slope is then given:

$$+ 2.13 \text{ and } - 2.36 \text{ degrees}$$

It should be noted here that actually two programs were run.
One held the slope or angle from the horizontal constant at 15.0
degrees and inquired the necessary voltages to maintain this value
assuming a linear continuous potential gradient in the direction of
ion travel. This gave the approximate voltage values to be on the
field wires. These values are approximate since the actual electric
field created in the region by the several wires and ground plate is
not continuous, but stepwise increasing.

The continuous program was used as a guide to set the voltages
on the wires and to estimate the potential gradient for the region
between the wires. These values were then used in the second pro-

gram to calculate the voltages on the wires so that the constant elec-
tric field in the region directly over the wires and the linearly in-
creasing field in the region between the wires would be such as to
yield values for the slopes of the ion trajectories as close to 15.0
degrees as possible. Several programs were written, based on the
solutions for the equations of motion and two of them are presented
in the Appendix. Also two pages of computer output data are pre-
sented there as typical examples.

It can be seen that the angular spread for the entire range
of velocities is only 4.49 degrees. Using the relation

$$\pi \text{ radians } = 180 \text{ degrees}$$

and (4.23)

$$\text{arc length} = r \ \theta \ ,$$

a conservative angular spread of 5.0 degrees yields an approximate
spread of only 0.873 cm after 10.0 cm of travel from the exit of the
electrostatic lens system, i.e.,

$$\text{arc length} = 10.0 \text{ cm X } 0.0873$$

$$\text{arc length} = \ 0.873 \text{ cm}$$

The diameter of the quadrupole aperture is 1.15 cm. This means
that at a distance of 10.0 cm, the quadrupole should be in a posi-
tion to accept all ions that pass through the lens in the prescribed
manner.

The field wires or electrodes are situated so that the separa-
tion between them and the base ground plate is constant at 4.0 cm.

The electrodes themselves are 0.5 mm in diameter and the longi-
tudinal center-to-center separation of the electrodes is 2.0 mm. The
electrodes are constructed of high purity nickel (Ni #200, 99%), as

is the base ground plate.

The voltage values for the five (5) electrodes as well as the potential gradients are shown in Table XI.

In this table, electrode number 1 corresponds to the wire electrode nearest to the entrance of the electrostatic lens. Electrode number 5 is very near the exit of the lens. ALPHA I corresponds to the potential gradient in the direction of ion travel, for values of displacement into the field of from 0.0 to 2.5 mm. ALPHA II corresponds to values in the 2.5 to 8.0 mm range.

Figure 15 is presented as a graphic illustration of the potential distribution on the five effective field electrodes. It may also be taken as proportional to the electric field strength in the region, since the distance from all the electrodes to the base ground plate is the same.

The curve number 1 represents the potential distribution of the lens electrodes necessary to direct ion number 1, or Al^{+1}, toward the aperture of the quadrupole mass filter. Curve number 2 represents the potential distribution necessary to direct ion number 2, or Al^{+3}, toward the quadrupole, etc.

A single power supply may be used to provide the different voltages to all five of the effective field electrodes, if an appropriate voltage divider is employed. Such a voltage divider is presented in Figure 16. For design purposes, only the first five specie of aluminum ions were considered. The voltage on the fifth effective electrode, necessary to curve the trajectory of the fastest Al^{+1} ion by 15 degrees, was calculated to be 125.0 volts. Therefore the highest voltage required of the power supply has been determined. The lower

TABLE XI

VOLTAGE VALUES AND POTENTIAL GRADIENTS

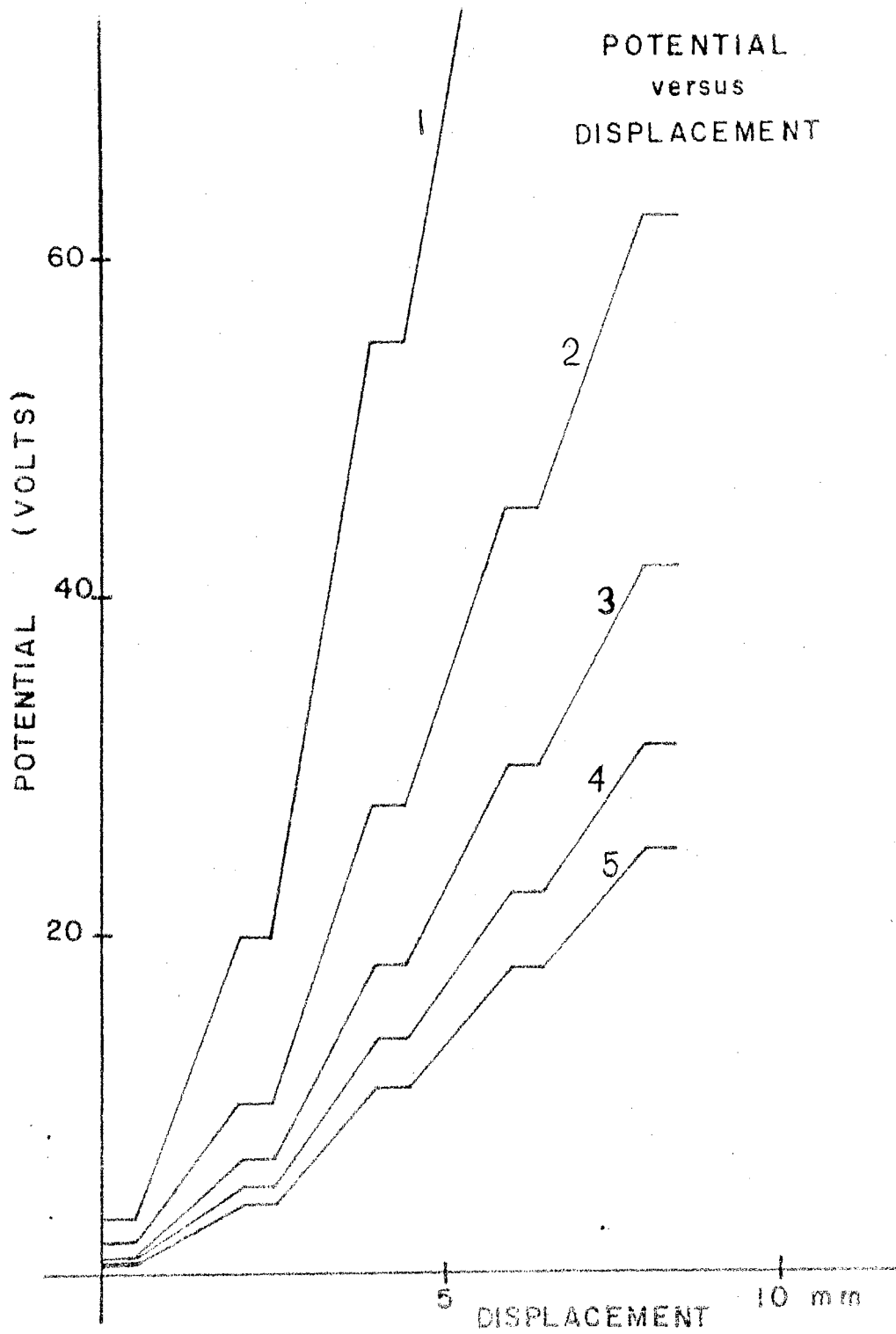| ION	ELECTRODE #1 volts	ELECTRODE #2 volts	ELECTRODE #3 volts	ELECTRODE #4 volts	ELECTRODE #5 volts	ALPHA I & II volts/mm	
1	3.00	20.00	55.00	90.00	125.00	8.947	18.420
2	1.50	10.00	27.50	45.00	62.50	4.474	9.210
3	1.00	6.67	18.33	30.00	41.67	2.982	6.140
4	0.75	5.00	13.75	22.50	31.25	2.237	4.605
5	0.60	4.00	11.00	18.00	25.00	1.789	3.684

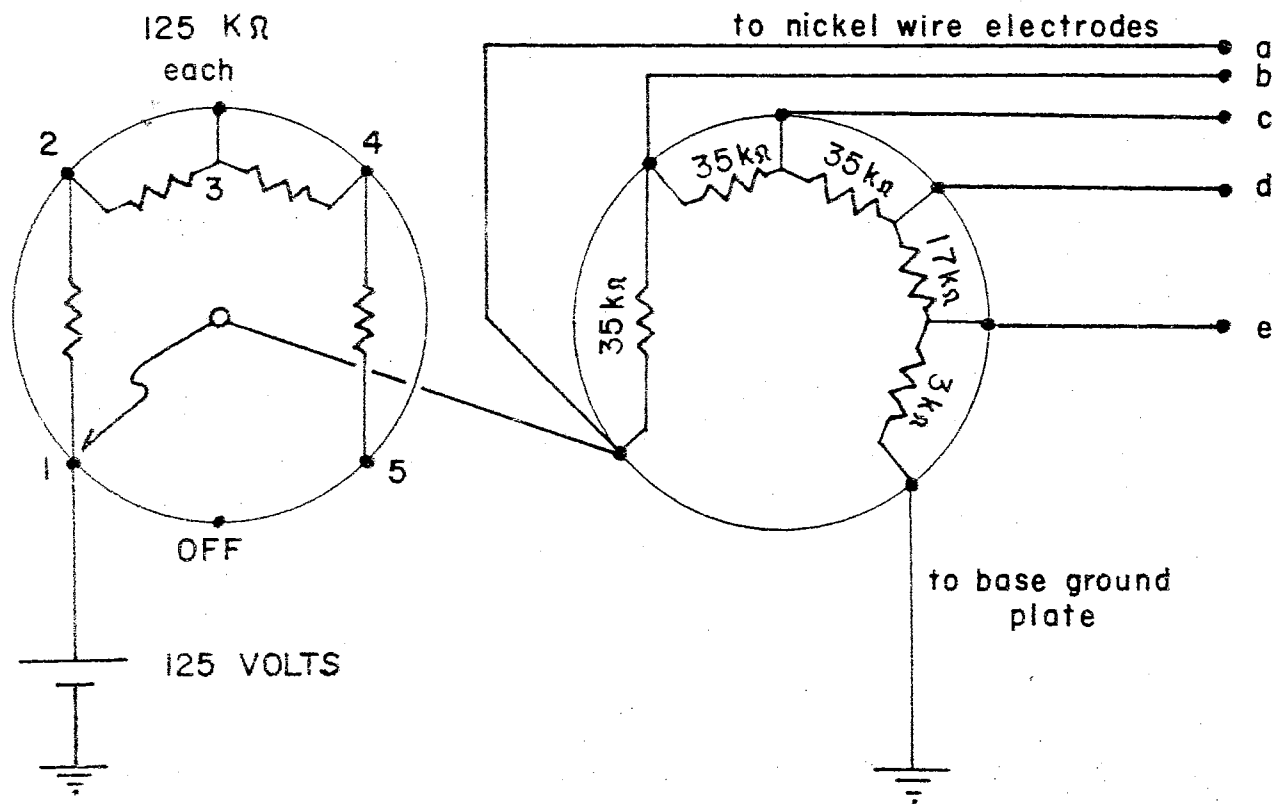Figure 15. Potential Profiles for Lens Electrodes

Figure 16. Voltage Divider for Electrostatic Lens Power Supply

voltages for the other electrodes are taken from the voltage divider.

The switch at the center of the left terminal block in Figure 16 is set for Al II, i.e., in the number 1 position. The terminal numbers on the switch correspond to the potential curves in Figure 15. The voltage divider output terminal letters correspond to the five effective field electrodes.

The position of the pulsed electrostatic lens, as it will be used to extract the ions from the plasma emission is shown in Figure 17. The plasma source, at the extreme right, emits a composition of light, neutral atoms and ions through the entrance slit. The light and neutral atoms pass through the lens undeflected, but the ions are accelerated directly at the quadrupole mass filter aperture.

Summary

The design and construction of the pulsed electrostatic lens has been completed and will soon be used as an integral part of the quadrupole mass filter assembly. The design of the pulsed power supply for the lens is under way and the delay circuits to synchronize the pulse with the arrival of the ions to the lens, are already available. In order to place a pulse of 125.0 volts for 1.0 microsecond on the voltage divider, which in turn, supplies the electrodes of the lens system, a Schmitt trigger circuit may be employed. The Schmitt trigger is a modified cathode-coupled bistable multivibrator, which is widely used as a voltage discriminator (Malmstadt and others, 1962). This trigger is useful as a "squaring circuit" and is often used in a sine-square generator to convert the output of a sine-wave oscillator to a square wave.
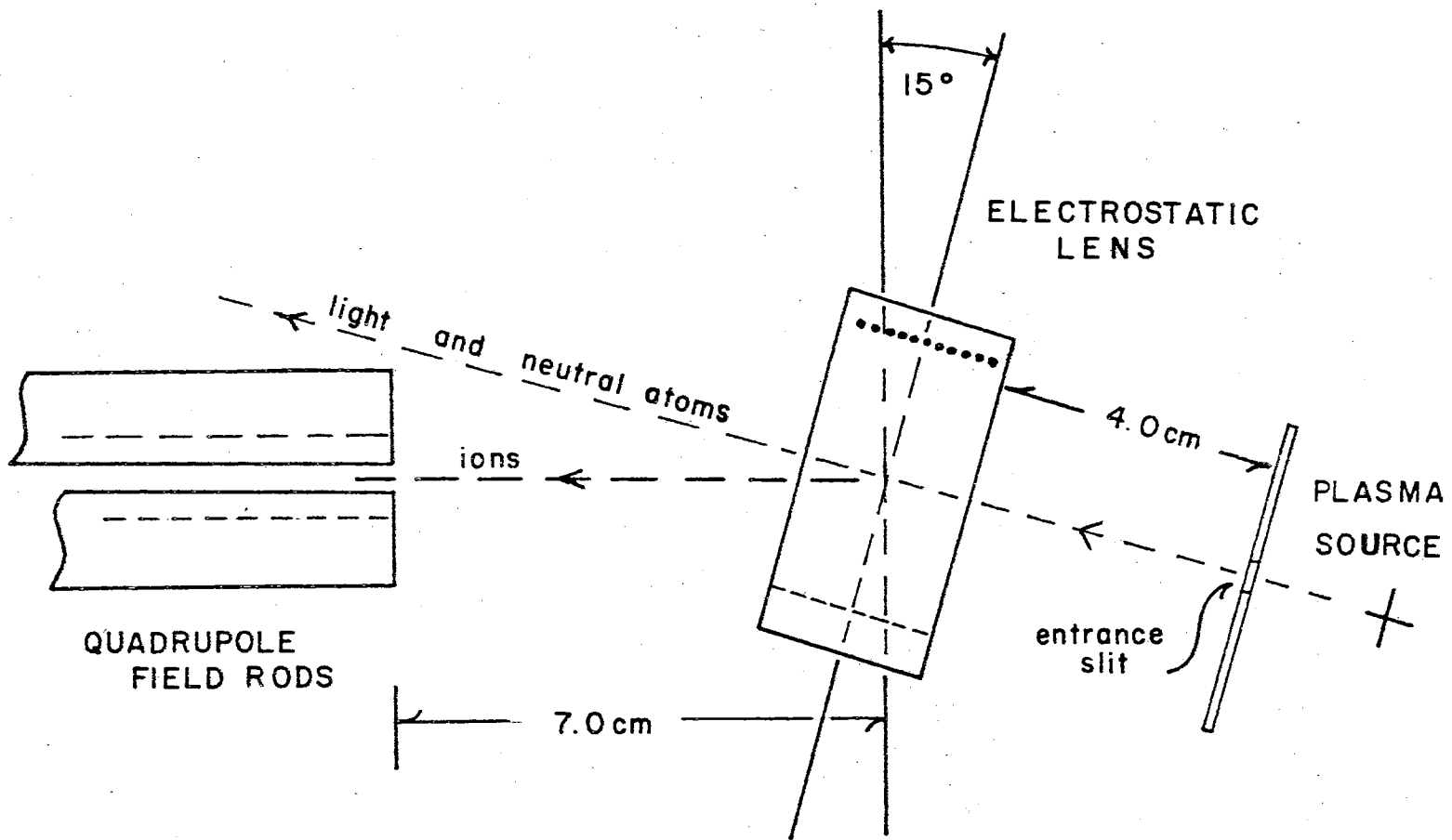
Figure 17. Electrostatic Lens in Operational Configuration

The vacuum spark discharge will be used to calibrate the delay system and to obtain proficiency in reducing the data. This data will be in the form of photographs, similar to the ones taken in the initial quadrupole experiments. It is hoped that with the electrostatic lens, velocity distributions of the ions from both the laser impact and the exploding wire plasmas can be obtained. The device should also enhance the resolution with which the relative ionic density of the plasma can be determined.

CHAPTER V

RESULTS AND CONCLUSIONS

The design and construction of the quadrupole mass filter assembly was completed in late 1967 and the preliminary testing began in early 1968. The mechanical components of the assembly behaved well, but some difficulty was encountered in constructing a stable, class "C" oscillator. Much effort was expended in balancing the oscillator circuits and it was found that additional trimmer capacitors were necessary for balance. A new oscillator tube that was defective added to the instability. Both oscillator tubes were replaced and the power supply was operational. The power supplies for the discharge condenser and the electron multiplier gave no difficulty.

The quadrupole lens and the electron multiplier were placed into the vacuum system and were then ready to analyze the plasma ions. The aluminum spark gap, used to produce the plasma, was the same one used by Vernon D. Brown in his measurements of the emitted light. Payne has used the same spark at the same rated voltage and current to obtain spectrographs of the emitted light in the far ultraviolet, i.e., spectral lines are identified as being from Al IV, Al V, etc. Measurements of the ion content have been taken for three settings of the voltage across the gap. The most reproducible data was obtained with the 1.0 microfarad condenser charged to 10,000 volts. This was the same rating that was employed by Brown and Payne for

67

their measurements.

Procedure

In a typical data run, the quadrupole power supply is turned on for a period of approximately 30 minutes to allow the oscillator and rectifier tubes to warm up. During this period, the oscilloscopes are also turned on so that they will become completely stabilized before they are needed. The aluminum electrodes are aligned in the glass vacuum manifold and the pressure of the system is constantly monitored to insure that approximately 10^{-5} Torr is maintained. Next, the electron multiplier is turned on and the voltage is set to about 800 volts.

The quadrupole power supply is then set at the proper rf and dc voltages to obtain a particular ion. The high voltage power supply is turned on and set at 10,000 volts in order to charge the condenser. This condenser is then allowed to discharge through the spark gap. The resulting trace on the output oscilloscope is photographed.

Discussion of Spark Discharge Data

The variables to be considered in analyzing the curves, which are shown in this chapter, are given below. The electron multiplier is electrically biased to receive no electrons, so that they are not considered. The variables are identified in the following list.

(1) Light from the spark breakdown

(2) Excited atoms which are neutral, i.e., atoms that have been excited to a metastable state

(3) Singly ionized aluminum ions

(4) Doubly ionized aluminum ions

(5) Triply ionized aluminum ions

(6) Quadruply ionized aluminum ions

(7) Quintuply ionized aluminum ions

The variables appear in different combinations which may be selected, in part, by changing the fields in the quadrupole mass filter and by chance location of the position on the tapered electrodes at which the spark occurs. Since the ions travel a known distance, which is approximately 34.0 cm, the initial arrival time of each specie of ion at the electron multiplier is indicated by the curves for that particular specie of ion. The initial response of the quadrupole mass filter is to the ultraviolet light from the spark and this is an accurate indication of time zero. The time interval which is measured between zero time and the arrival of 10 percent of the ions of one specie is the time that is required for the ions to traverse the distance of 34.0 cm. This velocity corresponds, to a first approximation, to the random velocity of the ions. If this assumption is accepted, the relation, $1/2 \, m \, v^2 = 3/2 \, k \, T$, permits one to know the (kinetic energy) temperature of the ions. The time of arrival of the different ions permits one to compare the temperature (kinetic energy) of the different ions and of the excited (metastable) atoms.

Provided the ions of different species, such as Al^{+2}, Al^{+3}, ..., and excited atoms, have the same random velocity, the discharge is in kinetic equilibrium. It is entirely feasible for the different specie to be in kinetic equilibrium although from the set of measurements that have been obtained for conditions equivalent to those of Payne and Brown, there cannot be equilibrium between the ionization energy

and the kinetic energy. Figure 18 gives the ionic energy as a func-
tion of the random velocity.

A considerable amount of information may be dedcued from the data,
and a considerable amount of interpretation is required. Some of the
problems in the interpretation have been encountered before in the
data from the spark breakdown, taken by Carpenter and Brown.

The shape of all the curves that are presented in Figure 19 is
controlled and dominated by the light emission. The electron multi-
plier responds by producing a current for ultraviolet photons, as
well as for some of the photons of shorter wavelength in the visible.
For the set of curves at the top of Figure 19, the lower solid curve
represents the light emission and provides a base curve for reference.
The curves superposed on the light emission provide a sample compar-
ison of all the ions with no ions. The curve for all ions was ob-
tained by turning the quadrupole fields completely off. Therefore
all ions, regardless of their charge, were allowed to pass through
the lens as there is no filtering action. The dotted curve represents
only neutral, metastable aluminum atoms and the light emission. To
obtain this curve, the quadrupole power supply was set at values for
which no ion could penetrate the field.

Several interesting features were illustrated for the light
emitted by the spark discharge. The curve for the light alone is ob-
tained occasionally and its occurrence is determined by chance. It
is believed that this curve results when the spark is such that the
ions are emitted away from the aperture of the quadrupole lens. Its
reproducibility with respect to the oscillations in the first few
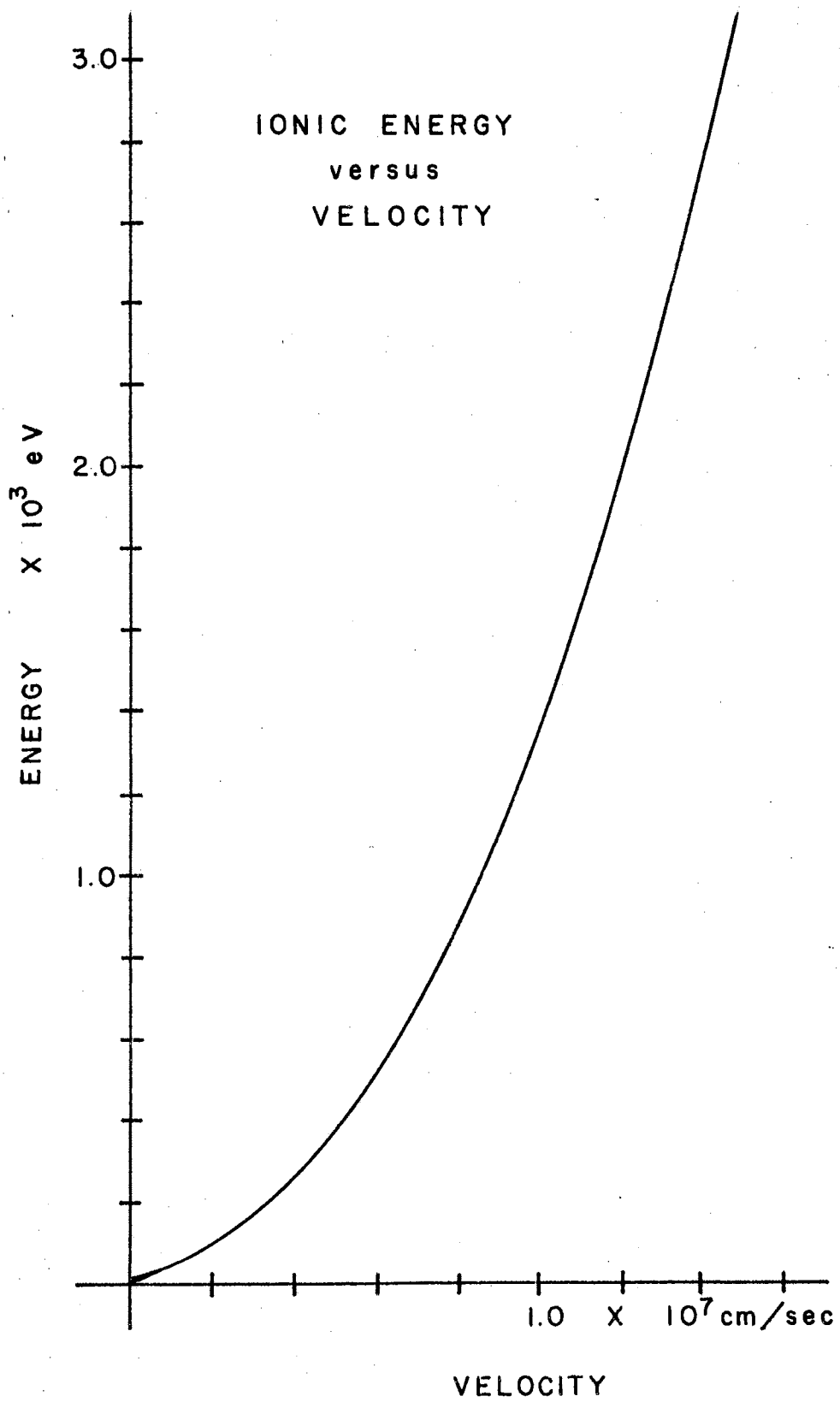microseconds and with respect to its amplitude, lend credence to this

Figure 18. Graph of Random Ionic Energy
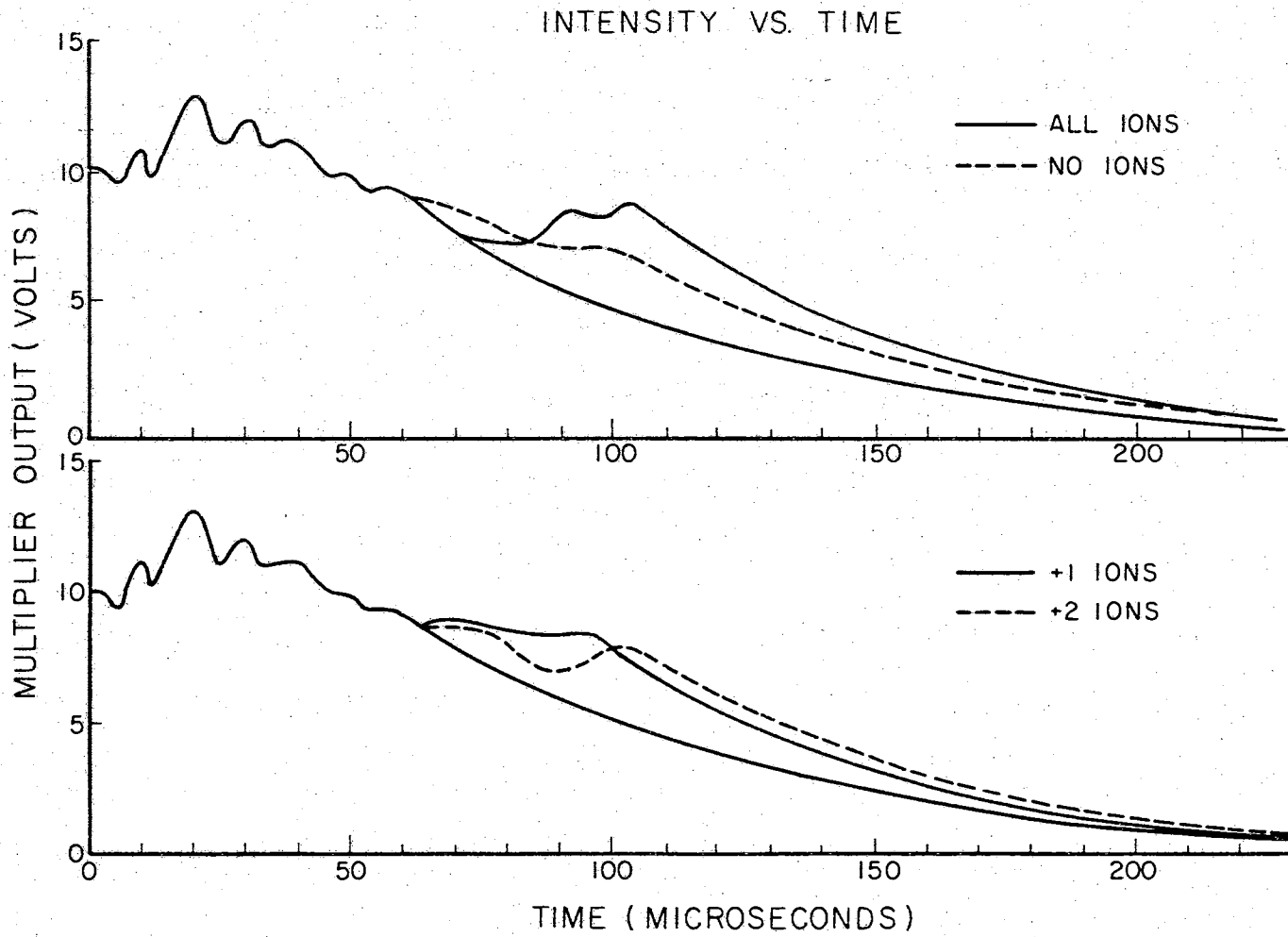Versus Velocity

INTENSITY VS. TIME

Figure 19. Spark Discharge Curves for Al, Al +1 and Al +2

interpretation. The first oscillation on these curves was masked by
noise and no attempt was made to interpret this region. From the curve
for the light emission, the plasma continues to emit light, as well as
ions, for the entire time that the curves were recorded, i.e., for
over 200 microseconds.

The oscillations have a duration of about 10 microseconds. Since
each half cycle of voltage should produce of power input, as in any
electric circuit, the frequency of the oscillation is about 50 khz.
This is the natural frequency for the condenser discharge through the
spark. These oscillations are of considerable amplitude for a period
of about 40 microseconds, which indicates that the condenser dis-
charge is completed in this time. This is significant for the forma-
tion of the stable plasma, since the plasma is not fully formed and
therefore is not very stable until the discharge is complete.

This interpretation finds some substantiation in the nonrepro-
ducible regions of the curves, where the arrival of the ions and
metastable atoms at the multiplier is first indicated. This region
of the curves is also of approximately 40 microseconds duration. This
duration corresponds very well, as it should, with the creation time
of the plasma.

Note that the ions and neutrals begin to arrive at the multi-
plier between 60 and 70 microseconds after the breakdown begins. The
intensity from the excited atoms and the ions is the difference be-
tween the ordinate of this curve and the ordinate for the photons.

On the lower set of curves in Figure 19, it is readily seen
that the base for the photon emission is practically identical to that
in the upper set. The dotted curve corresponds to the Al^{+1} ions,

whereas the solid curve represents the Al^{+2} ions. It must be remembered that the neutrals are also included in these amplitudes. The curves are so designated because the voltage parameters "a" and "q" have been set to select only the Al^{+1} and Al^{+2} ions, respectively. Maximum amplitude is attained for each ionic specie when the voltages are set at the calculated values.

The random velocities of the ions and/or the metastable atoms may be taken, to a good approximation, directly from the Intensity versus Time plots. In the upper set of curves, velocities of the order of 5 X 10^5 centimeters per second were recorded for metastable atoms, while velocities of 4 X 10^5 centimeters per second and lower are shown in the figure for the all-ions configuration.

Both the Al^{+1} and Al^{+2} curves indicate ionic velocities of the order of 5 X 10^5 centimeters per second, which corresponds to an energy of 3.5 eV. It must again be emphasized that this measured value is considerably higher than would be expected in the plasma proper. The measured value of 6.0 eV corresponds roughly to a plasma energy of the order of one (1) eV, or a temperature of approximately 12,000 Kelvin degrees.

Additional information on other ionic species is given in Figure 20. The set of curves at the top of this figure compare Al^{+3} with Al^{+4} and a measure of Al^{+5} is presented in the lower set. The presence of these specie is firmly established by the interpretation of the emitted spectra in the far ultraviolet by Carpenter.

As of this writing, no quantitative evidence is available from the quadrupole data to substantiate the qualitative conclusion that the specie, Al^{+3} is the most abundant. However, measurements with the
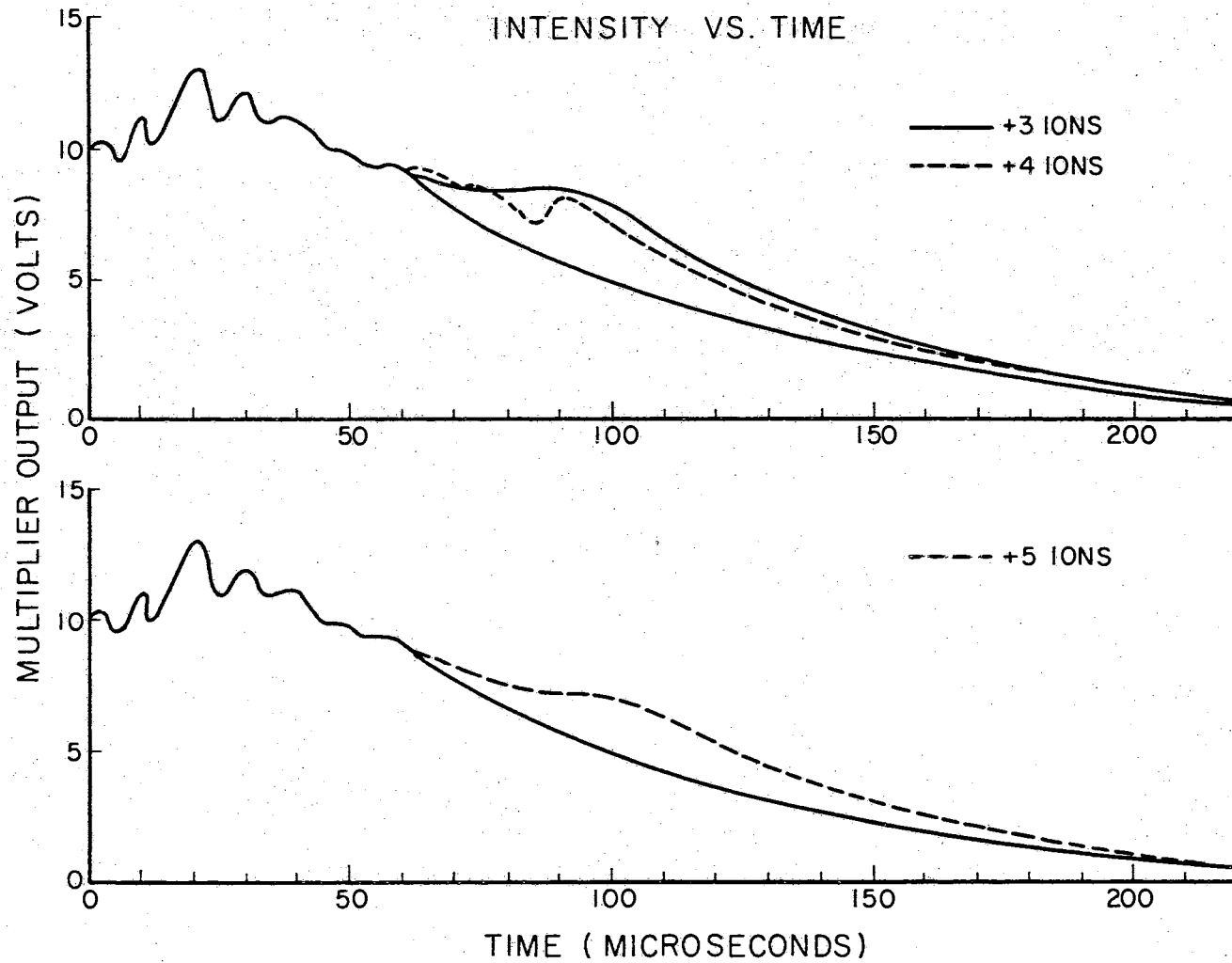
Figure 20. Spark Discharge Curves for Al +3, Al +4 and Al +5

spectrograph appear to support this preliminary evaluation of the data.

Discussion of Laser Impact Data

The quadrupole mass filter was employed to analyze the emission of ions and light from an aluminum plasma that was produced by laser beam impact. The design and construction of the laser was completed by Peery (1967). Mr. W. G. Robinson made modifications on the laser assembly and through his efforts, operation in the Q-switched mode was achieved. The laser is fired by charging a large condenser bank with a high voltage power supply and then allowing the bank to discharge through helical flash lamps. These lamps optically excite the twin ruby rods. The resulting giant laser beam is then focused onto the aluminum target. The plasma, thus created, is allowed to expand freely into a vacuum. The ions, metastable atoms and the light emission is monitored with the quadrupole mass filter.

The aluminum target was positioned, in vacuum, so that approximately the same drift space existed as that for the spark discharge. Since the plasma is produced in about 30 nanoseconds and emission in the ultraviolet continues for only about 2 microseconds, the curve may, with some hesitation, be interpreted as velocity distributions. It is not clear as to the meaning of a lack of emission during the time of flight. The pressure of the vacuum chamber, containing the aluminum target, was maintained at about 10^{-5} Torr.

Some typical examples of the data obtained with the quadrupole in the initial analysis of the plasma, produced by the laser, are presented in the following figures. The dominating feature in Figure 21 is the ultraviolet light emission. The peak amplitude of this
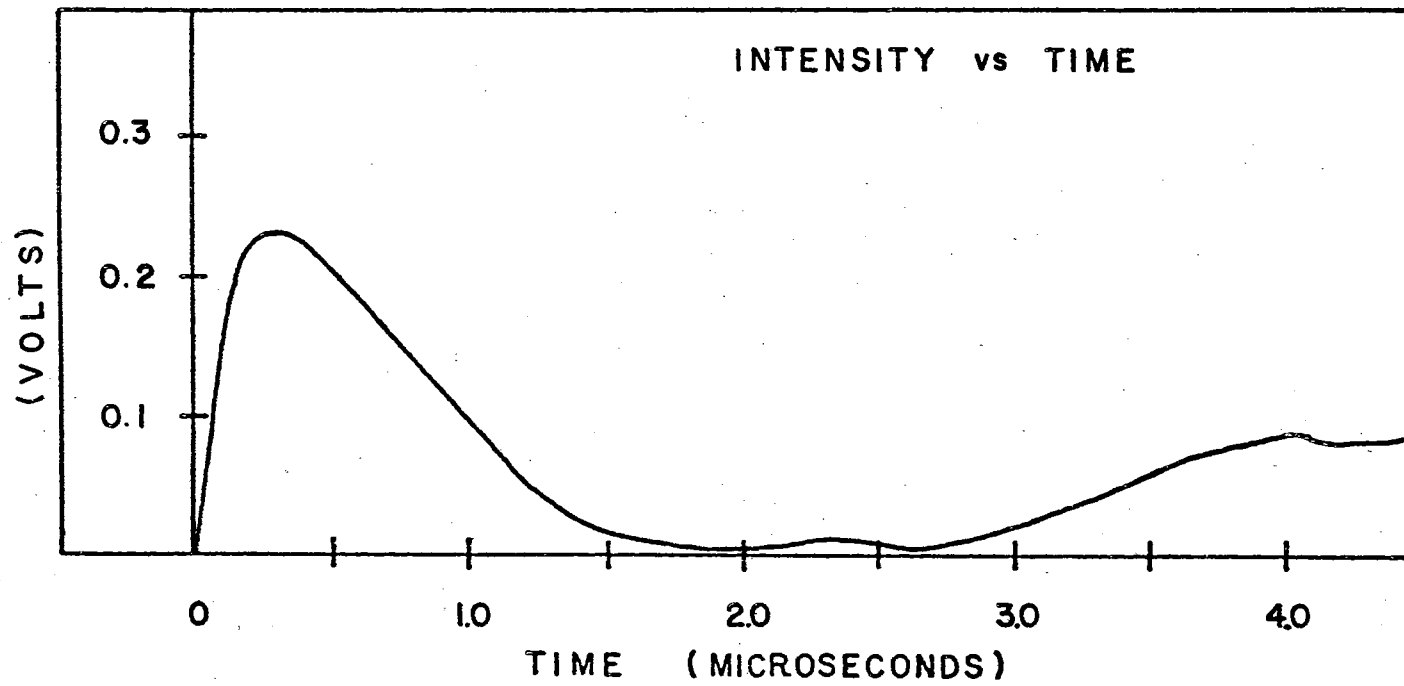
Figure 21. Laser Impact Emission of All Aluminum Ions, Metastable Atoms and Light

emission is reached after about 0.25 microsecond and it has decayed to nearly zero amplitude after 2.0 microseconds. This emission duration is significant since it may very well indicate the production time of the plasma. To obtain this curve, the quadrupole power supply was turned completely off, allowing all specie of ions to pass through the mass filter along with the metastable atoms and light.

Figure 22 shows a curve obtained under similar conditions, but with the time scale increased by a factor of ten. Notice first of all that what is believed to be the ultraviolet emission cut-off also occurs at approximately 2.5 microseconds. What is considered to be the initial burst of ions begins immediately after the decay of the light emission, or at about 2.0 to 2.5 microseconds after impact.

Figure 23 is presented for comparison with the subsequent curves and is a result of similar conditions as for Figures 21 and 22, but with an increased voltage scale.

The quadrupole was set to reject all ions except Al^{+2} and the laser was fired in the usual manner. The resulting trace, shown in Figure 24, gives an indication of the Al^{+2} ions, metastable atoms and light.

Two curves are presented for Al^{+3} in Figures 25 and 26. A comparison of these will show that while the data is highly reproducible with respect to the initial light emission and the arrival of the first ions and/or neutrals, the obvious difference in amplitudes indicates that no two impact phenomena are identical, however, similar they are.

An indication of the Al^{+4} ions is shown in Figure 27.

The variance in the amplitudes of the curves for identical
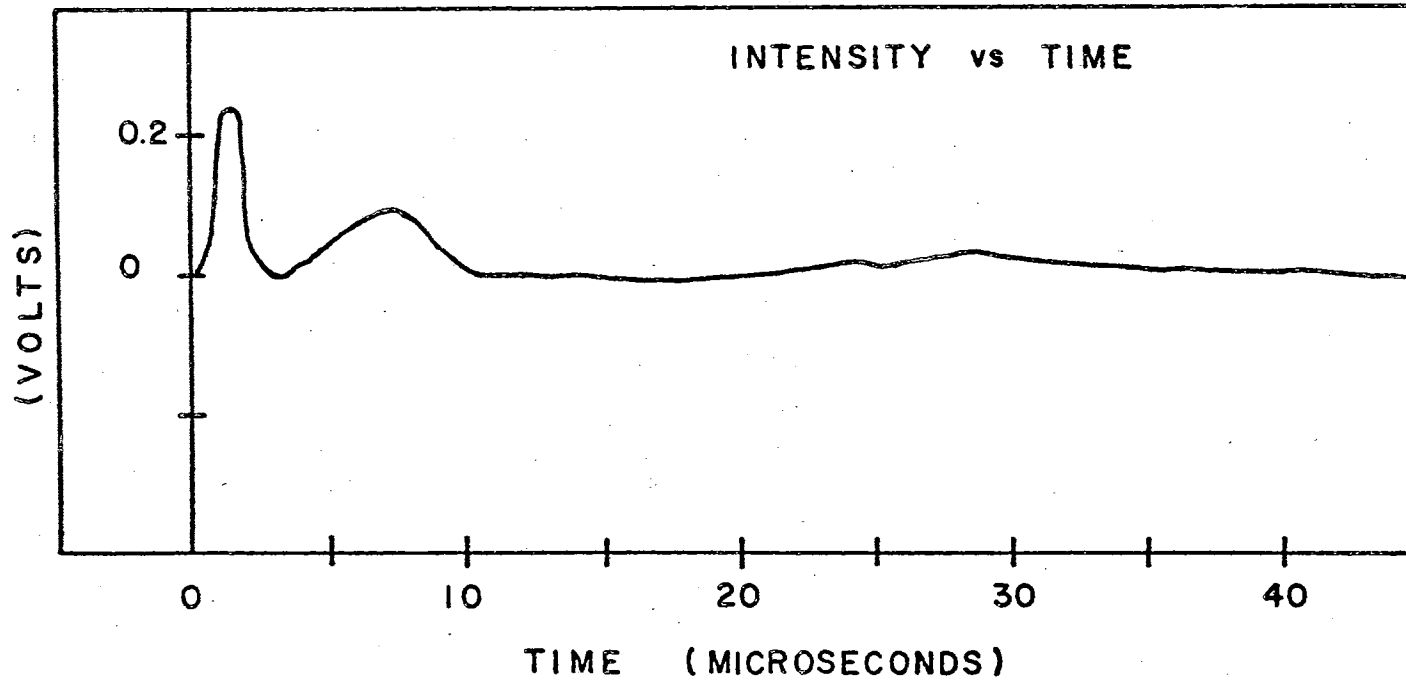
Figure 22. Laser Impact Emission of All Aluminum
Ions, Metastable Atoms and Light on
Increased Time Scale

Figure 23. Laser Impact Emission of All Aluminum
Ions, Metastable Atoms, and Light
on Increased Voltage Scale

Figure 24. Laser Impact Emission of Al +2, Metastable Atoms and Light
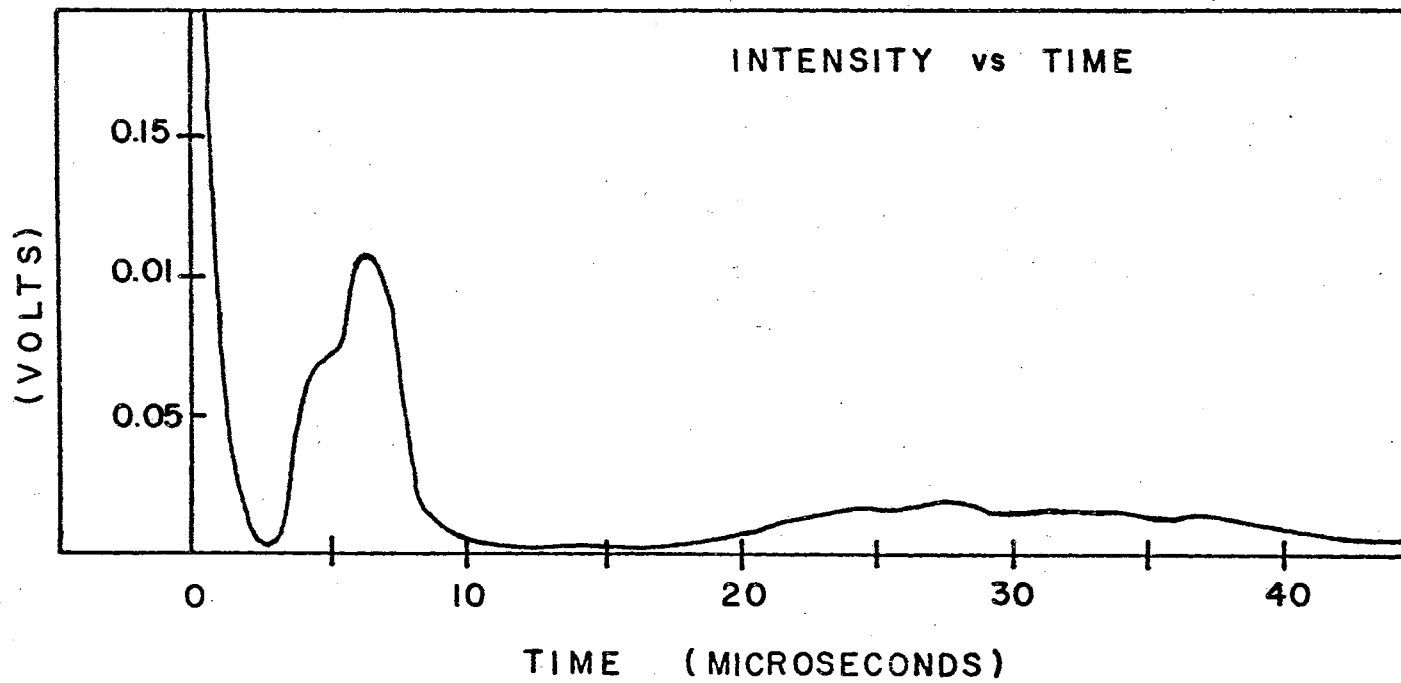
Figure 25. Laser Impact Emission of Al +3, Metastable Atoms and Light
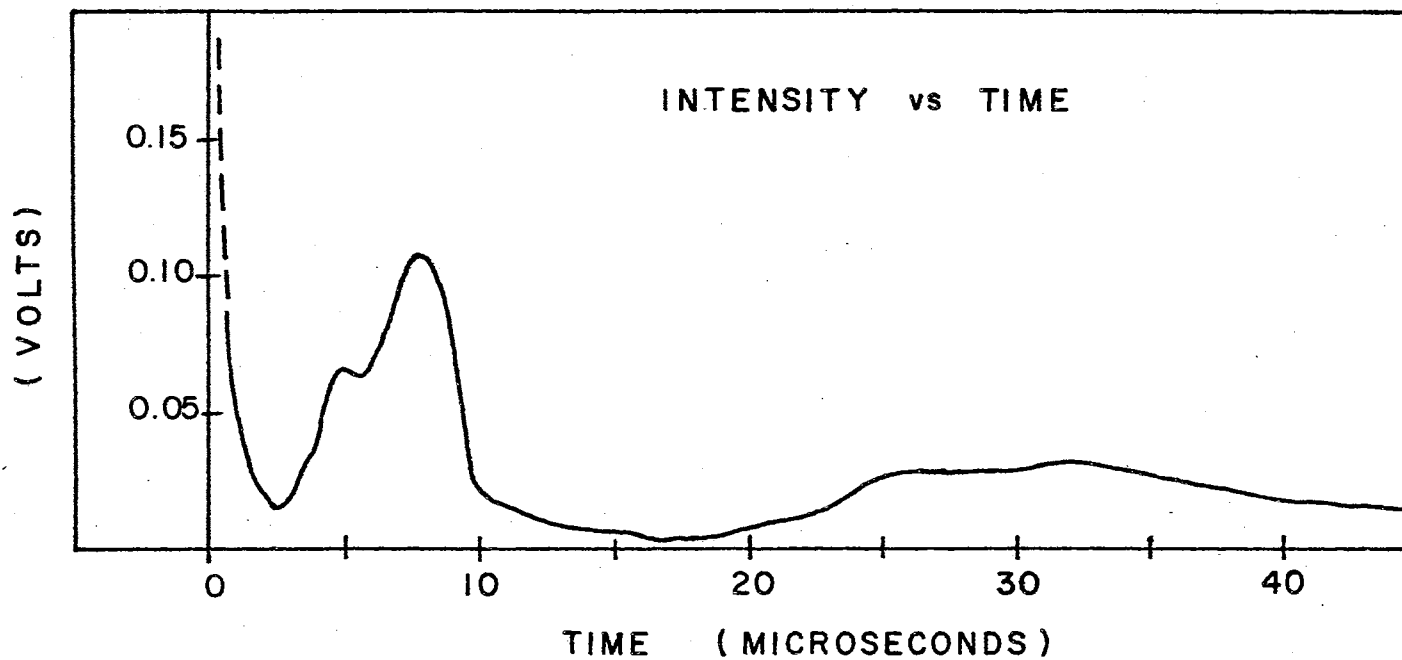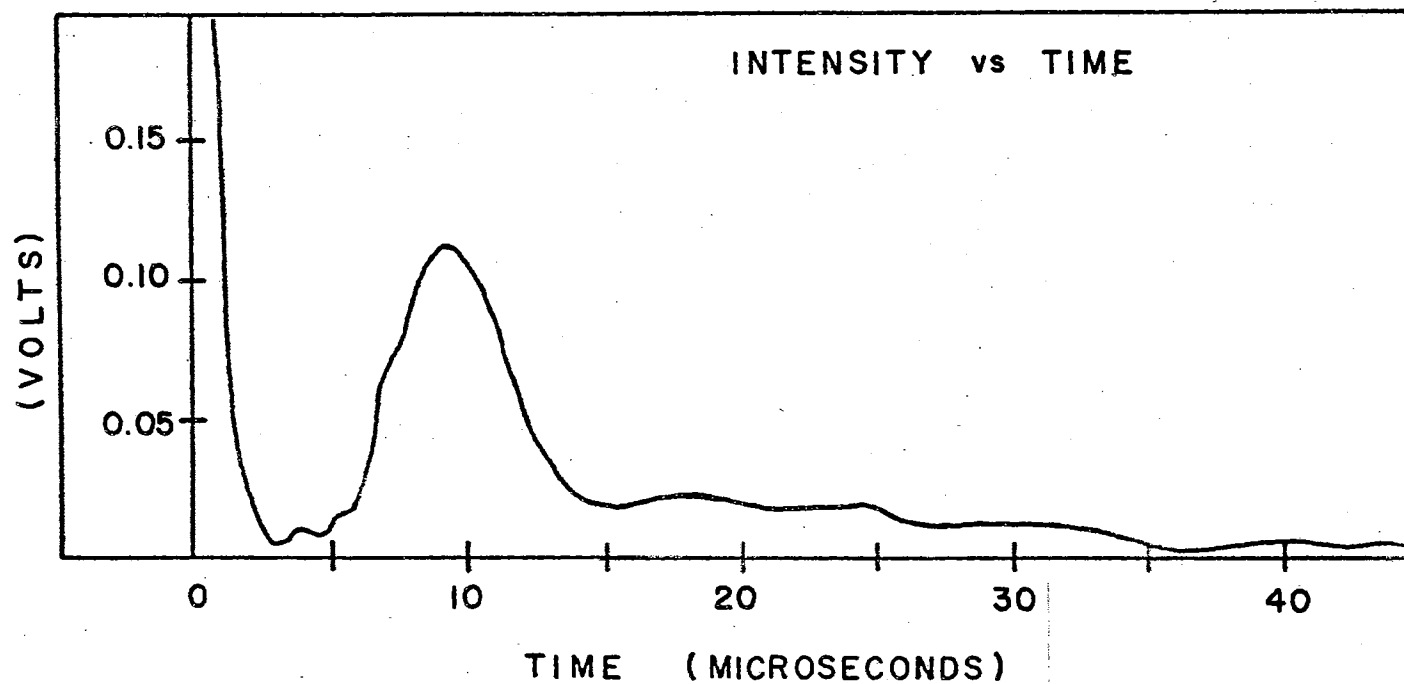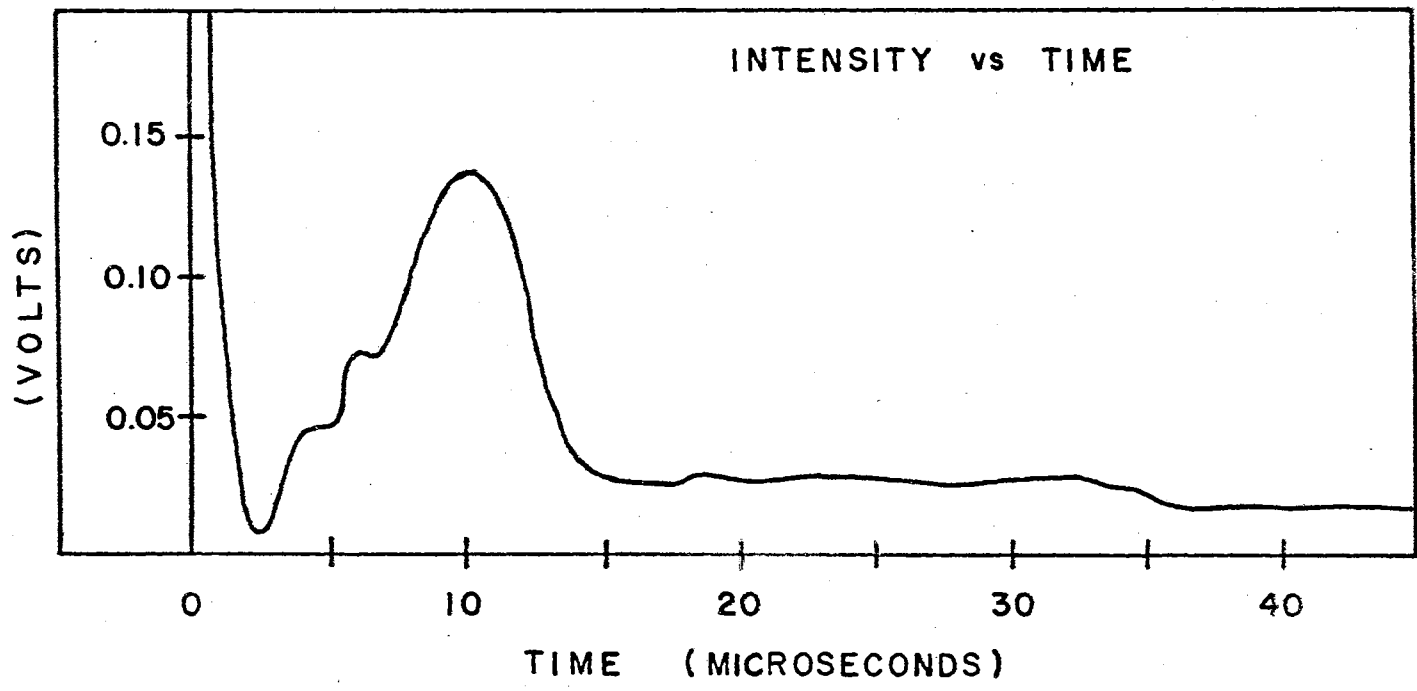
Figure 26. Laser Impact Emission of Al +3, Metastable Atoms and
Light Indicating Increased Ionic Concentration
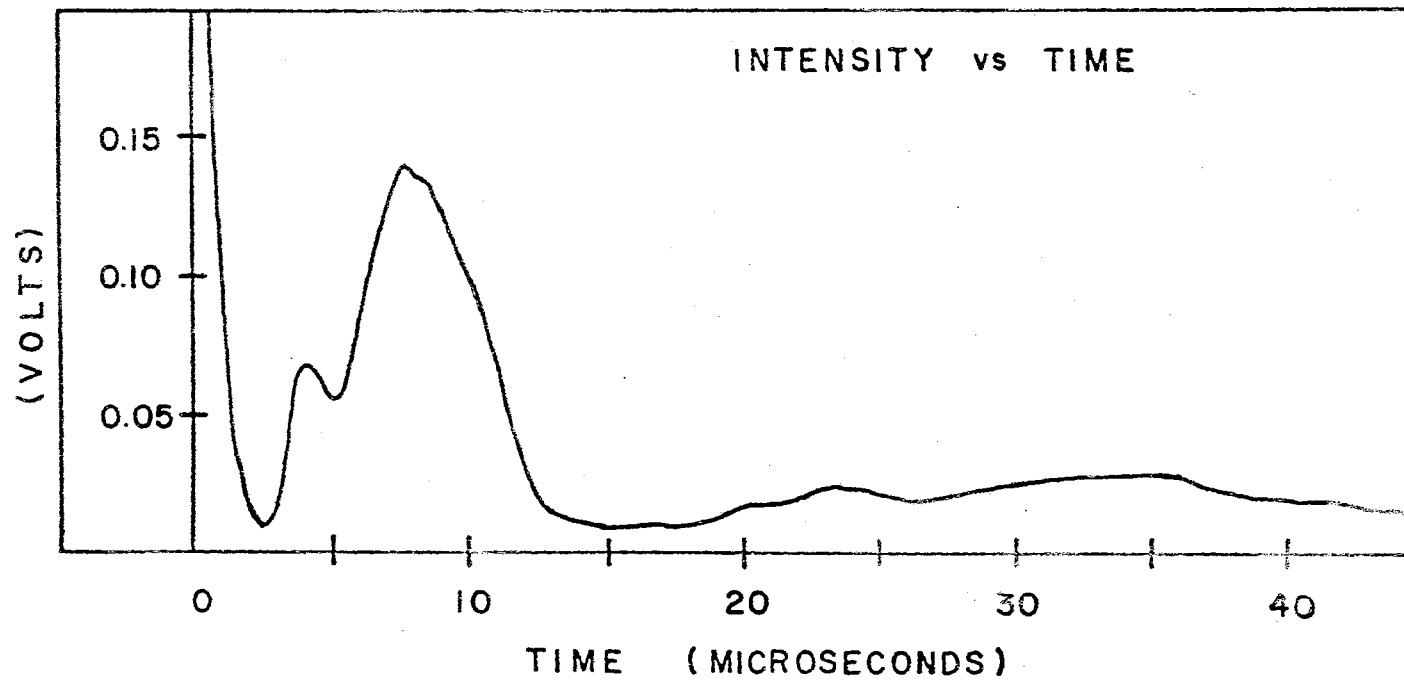
Figure 27. Laser Impact Emission of Al +4, Metastable Atoms and Light

quadrupole field values will necessitate a statistical a statistical

evaluation of the data, with regard to the relative concentration of

each specie, but from the curves presented here, significant informa-

tion regarding the velocities of the ions and neutral atoms may be

gathered.

If the peak, beginning at 2.5 microseconds in Figure 23, may be

accurately designated as the arrival of aluminum ions from the target

area, then their velocity has a measured value of the order of 10^7

centimeters per second. This velocity corresponds to an energy of

1.4 keV and a Boltzmann temperature of 10,800,000 Kelvin degrees.

The burst of ions corresponding to the peak beginning at about 20

microseconds, yields values for the velocity of the order of 1.7×10^6

centimeters per second. Velocities of approximately this value cor-

respond to ionic energies of between 20 and 50 eV and to temperatures

in the 300,000 Kelvin degree range.

Observations of the continuous spectrum from the sun and the ap-

plication of the laws of radiation indicate that the effective,

surface temperature of the sun is about 6,000 Kelvin degrees. Dr.

L. W. Schroeder, of the Astrophysics Group at Oklahoma State Uni-

versity, indicates that the interior temperatures of the sun have

been reported to be of the order of 15 to 20 Kelvin degrees. Using

these values as a yard stick, the extremely high temperatures of the

plasma may be appreciated.

The study of sodium plasmas, carried out by researchers at the

Honeywell Corporate Research Center, Hopkins, Minnesota, has pro-

duced plasma energies of 20 to 30 eV (ready, 1967). These results

correspond to temperatures in the 300,000 degree range, measured in

Dr. Todd's group here at Oklahoma State.

Summary

The results of the quadrupole mass filter analysis of the spark discharge and the laser impact have provided some experimental verification of the theoretical work, currently being done by this group. The work has not only been rewarding in terms of the initial results, but the results themselves have provided an incentive to further investigate the properties of transient plasmas.

It is hoped that in the near future, an analysis of the exploding wire plasma may give an even better understanding of the behavior of the ions, metastable atoms and light. The exploding wire assembly was constructed by Mr. J. A. Yoder and tests are currently being made to determine its operational characteristics.

One major advantage the exploding wire offers is the very short production time of the plasma. A production time of the order of 1.0 microsecond will not only decrease the uncertainty with which velocity distribution measurements can be made, but it presents the possibility of attaining a plasma in equilibrium. The two other methods of plasma production, mentioned in this report, do not.

Other planned experiments include the addition of the pulsed electrostatic lens to the quadrupole assembly. The exciting prospect of analyzing the individual ion velocity distributions with the aid of this device promises to make a major contribution to the state of the art of plasma physics.

SELECTED BIBLIOGRAPHY

Allen, James S. "The Detection of Single Positive Ions, Electrons
    and Photons by a Secondary Electron Multiplier." Physical
    Review, Vol. 55 (1939) pp. 966-971.

Brown, Vernon D. and F. C. Todd. "Use of a Pulsed Photomultiplier to
    Measure the Light Intensity versus Time for a Spark Discharge
    Between Aluminum Electrodes." (unpublished Ph.D. dissertation,
    Oklahoma State University, 1968).

Brubaker, W. M. and J. Tuul. "Performance Studies of a Quadrupole
    Mass Filter." Rev. Sci. Inst., Vol. 35 (1964) pp. 1007-1010.

Carpenter, T. Milton and F. C. Todd. (unpublished M. S. report,
    Oklahoma State University, 1967).

Compton, K. T. and Irving Langmuir. "Electrical Discharges in
    Gases." Review of Modern Physics, Vol. II (April, 1930).

Dawson, P. H. and N. R. Whetten. "Quadrupoles, Monopoles and Ion
    Traps." Research and Development, (February, 1968) pp. 46-50.

Gartenhaus, Solomon. Elements of Plasma Physics. New York: Holt,
    Rinehart and Winston, 1964.

Gunther, Karl-Georg. "A Partial Pressure Vacuum Gauge Working
    According to the Principle of the Electrical Mass Filter."
    Vacuum, Vol. 10 (1960) pp. 293-308.

Hellund, E. J. The Plasma State. New York: Reinhold Publishing
    Corporation, 1961.

Langmuir, I. and L. Tonks. Physical Review, Vol. 33 (1929) pp. 195,
    990.

Malmstadt, H. V. and C. G. Enke. Electronics for Scientist. New
    York: W. A. Benjamin, Inc., 1962.

McLachlan, N. W. Theory and Application of Mathieu Functions. New
    York: Dover Publications, Inc., 1964.

Mosharrafa, M. and H. J. Oskam. "Design and Construction of a Mass-
    Spectrometer for the Study of Basic Processes in Plasma Physics."
    (Tech. Rep. No. 2, AD-274249, University of Minnesota, 1961).

Norgren, Carl T. and others. Colloid Thrustor Beam Analysis; Design

and Operation of a Suitable Quadrupole Mass Filter. Lewis Research Center, NASA TN D-3036, Cleveland, Ohio, 1965.

Paul, W. and M. Raether. "Das Electrische Massenfilter." Zeit. fur Phys., Vol. 140 (1955) pp. 262-273.

Paul, W. and H. Steinwendel. "Ein Neues Massenspektrometer ohne Magnetfeld." Zeit. Naturforschg. Vol. 82 (1953).

Payne, R. D. and F. C. Todd. "A Spectrograph for the Far Ultraviolet," Proc. Okla. Acad. Sci., Vol. 46 (1966) pp. 115-121.

Peery, Larry J. and F. C. Todd. "Design and Construction of a Twin Ruby Laser." (unpublished M. S. thesis, Oklahoma State University, 1967).

Ready, John F. (Private Communication, 1967).

Woodward, C. E. and C. K. Crawford. "Design of a Quadrupole Mass Spectrometer." (Tech. Rep. No. 176, NP-12543, Mass. Inst. of Tech., 1963).

APPENDIX

The equations of motion for the ions that traverse the electro-
static lens are given in Chapter IV. Because of the many calculations
to be made to determine the field dimensions and the voltage values
for the lens electrodes, two computer programs were written so that
the behavior of the ions could be determined for a variety of initial
conditions. Among these conditions are included the electric field
width, the field length, the diameter of the lens electrode wires,
the spacing of the wires and the voltage to be applied to each elec-
trode. Also a factor, which was considered in the calculations, was
the electric field gradient in the direction of ion travel. It should
be noted that several pulse intervals, from 1.0 to 10.0 microseconds,
were considered. The best solutions were obtained for 1.0 micro-
second.

The programs were written in the FORTRAN IV computer language
and were run on the IBM 360 computer, model 50.

Continuous Program

The initial programs were written to inquire of the equations
of motion, the positions and slopes of the ions after a predetermined
time in the field. In this type program, the electric field was
specified as continuously increasing in the direction of ion travel.
Several values of the field were introduced in the program to obtain
exit slopes that were consistent with the geometry of both the pro-

posed lens and that of the existing quadrupole. It must be remembered
that the field gradient is the factor involved for extracting the ions
from the lens at the same angle. The electric field, necessary to
deflect a slow ion a given angle will hardly affect the trajectory
of an ion whose velocity is a factor of ten greater. Since all the
ions, regardless of their velocity, must pass through the same field,
the field value at the end of the lens must be large enough to deflect
the faster ions the same angle as the lower field, at the front of
the lens deflects the slower ions. Also this field must be turned
off by the time the slower ions reach the end of the lens so they
will not be deflected further.

A typical program of the continuous type is presented in Table
XII. A sample page of the computer output for this program is pre-
sented in Table XIII. For this program, the velocity ranged from
700 to 7000 meters per second in 10.0 meter per second intervals. It
is assumed that all ions, regardless of their velocity are present
at $x = 0$ for $t = 0$. This point represents the entrance to the lens.
It will be noticed in this program that the slope, or angle THETA, is
held constant at 15.0 degrees. The program then gives the voltage
values along the route of ion travel which are necessary to give the
15.0 degree deflection. In the illustration given, the potential is
specified at the point the ions have reached at the end of the 1.0
microsecond interval. The value of the field gradient at this same
point is also specified.

Discontinuous Program

The values of the field gradient from the continuous program

TABLE XII

TYPICAL CONTINUOUS PROGRAM FOR ELECTROSTATIC LENS

```
      $JOB 2233-40031 H WAYNE WILLIS
   1      1 FORMAT(////,2X,5HAN = ,E10.4,3X,5HAK = ,E10.4,3X,4HT = ,E10.4,3X,
          16HPTO = ,E10.4,3X,4HV = ,E10.4,3X,5HDV = ,E10.4,3X,5HVF = ,E10.4,
          2/,3X,4HW = ,E10.4,20X,8HALPHA = ,E10.4)
   2      2 FORMAT(/,4X,I4,5X,6(E12.4),22X,E12.4)
   3      3 FORMAT(///,7X,1HM,10X,1HY,11X,1HS,9X,5HTHETA,8X,2HPT,11X,1HX,11X,
          15HALPHA,35X,1HV)
   4      4 FORMAT(5X,E10.4)
   5        READ(5,4) AN,AK,T,PTO,V,DV,VF,W,ALPHA
   6      9 WRITE(6,1) AN,AK,T,PTO,V,DV,VF,W,ALPHA
   7        V=7.0E 02
   8        M=1
   9        DVO=DV
  10        PT=PTO
  11     10 WRITE(6,3)
  12     11 X=V*T
  13        S=((AN*AK)*(2.0*PTO*X+ALPHA*X*X))/(V*V*W)
  14        Y=((AN*AK)*(PTO*X*X+ALPHA*(X*X*X)/3.0))/(V*V*W)
  15        THETA=ATAN(S)*57.29578
  16        PT=PTO+ALPHA*X
  17        WRITE(6,2) M,Y,S,THETA,PT,X,ALPHA,V
  18        M=M+1
  19        IF(V.GE.VF) GOTO 50
  20        IF(V.GE.1000.0) DVO=10.0*DV
  21        V=V+DVO
  22        GOTO 11
  23     50 IF(AN.GE.5.0) GOTO 60
  24        AN=AN+1.0
  25        IF(AN.EQ.2.0) ALPHA=3.0 E 03
  26        IF(AN.EQ.3.0) ALPHA=2.0 E 03
  27        IF(AN.EQ.4.0) ALPHA=1.5 E 03
  28        IF(AN.EQ.5.0) ALPHA=1.2 E 03
  29        GOTO 9
  30     60 STOP
  31        END
```

$ENTRY

TABLE XIII

SAMPLE COMPUTER OUTPUT FOR CONTINUOUS PROGRAM

AN = 0.3000E 01   AK = 0.1786E 07   T = 0.1000E-05   PTO = 0.5000E 00   V = 0.7000E 04   DV = 0.1000E 02   VF = 0.7000E 04
W = 0.4000E-01   S = 0.2679E 00

M	Y	S	THETA	PT	X	ALPHA	V
1	0.8483E-04	0.2679E 00	0.1500E 02	0.9000E 00	0.7000E-03	0.5714E 03	0.7000E 03
2	0.8573E-04	0.2679E 00	0.1500E 02	0.9200E 00	0.7100E-03	0.5915E 03	0.7100E 03
3	0.8662E-04	0.2679E 00	0.1500E 02	0.9400E 00	0.7200E-03	0.6111E 03	0.7200E 03
4	0.8751E-04	0.2679E 00	0.1500E 02	0.9600E 00	0.7300E-03	0.6301E 03	0.7300E 03
5	0.8841E-04	0.2679E 00	0.1500E 02	0.9800E 00	0.7400E-03	0.6486E 03	0.7400E 03
6	0.8930E-04	0.2679E 00	0.1500E 02	0.1000E 01	0.7500E-03	0.6667E 03	0.7500E 03
7	0.9019E-04	0.2679E 00	0.1500E 02	0.1020E 01	0.7600E-03	0.6842E 03	0.7600E 03
8	0.9109E-04	0.2679E 00	0.1500E 02	0.1040E 01	0.7700E-03	0.7013E 03	0.7700E 03
9	0.9198E-04	0.2679E 00	0.1500E 02	0.1060E 01	0.7800E-03	0.7179E 03	0.7800E 03
10	0.9287E-04	0.2679E 00	0.1500E 02	0.1080E 01	0.7900E-03	0.7342E 03	0.7900E 03
11	0.9376E-04	0.2679E 00	0.1500E 02	0.1100E 01	0.8000E-03	0.7500E 03	0.8000E 03
12	0.9466E-04	0.2679E 00	0.1500E 02	0.1120E 01	0.8100E-03	0.7654E 03	0.8100E 03
13	0.9555E-04	0.2679E 00	0.1500E 02	0.1140E 01	0.8200E-03	0.7805E 03	0.8200E 03
14	0.9644E-04	0.2679E 00	0.1500E 02	0.1160E 01	0.8300E-03	0.7952E 03	0.8300E 03
15	0.9734E-04	0.2679E 00	0.1500E 02	0.1180E 01	0.8400E-03	0.8095E 03	0.8400E 03
16	0.9823E-04	0.2679E 00	0.1500E 02	0.1200E 01	0.8500E-03	0.8235E 03	0.8500E 03
17	0.9912E-04	0.2679E 00	0.1500E 02	0.1220E 01	0.8600E-03	0.8372E 03	0.8600E 03
18	0.1000E-03	0.2679E 00	0.1500E 02	0.1240E 01	0.8700E-03	0.8506E 03	0.8700E 03
19	0.1009E-03	0.2679E 00	0.1500E 02	0.1260E 01	0.8800E-03	0.8636E 03	0.8800E 03
20	0.1018E-03	0.2679E 00	0.1500E 02	0.1280E 01	0.8900E-03	0.8764E 03	0.8900E 03
21	0.1027E-03	0.2679E 00	0.1500E 02	0.1300E 01	0.9000E-03	0.8889E 03	0.9000E 03
22	0.1036E-03	0.2679E 00	0.1500E 02	0.1320E 01	0.9100E-03	0.9011E 03	0.9100E 03
23	0.1045E-03	0.2679E 00	0.1500E 02	0.1340E 01	0.9200E-03	0.9130E 03	0.9200E 03
24	0.1054E-03	0.2679E 00	0.1500E 02	0.1360E 01	0.9300E-03	0.9247E 03	0.9300E 03
25	0.1063E-03	0.2679E 00	0.1500E 02	0.1380E 01	0.9400E-03	0.9362E 03	0.9400E 03
26	0.1072E-03	0.2679E 00	0.1500E 02	0.1400E 01	0.9500E-03	0.9474E 03	0.9500E 03

were used as guides for simulating this field as closely as possible with a discontinuous field. It should be explained here that the field is discontinuous, so far as the field gradient is concerned. This results from the use of the discrete electrodes, instead of a single continuous one, to produce the high gradients necessary. The value of the field, directly over the electrodes, is approximately uniform and constant. The value of the field between the electrodes is very nearly linearly increasing. By the judicious appointment of voltages to the individual electrodes, the field values and gradients of the continuous case were closely simulated. This is to say that these values were calculated, using the computer programs, which were necessary to deflect the ions approximately 15.0 degrees from the direction of entry. A typical discontinuous program is presented in Table XIV. For these programs, the ions are considered to traverse, not one, but several electric fields as they pass through the lens. Because of this, the initial conditions at the beginning of each new field must be provided for each ion of a different charge and velocity. For all the ions, the initial conditions at the first field were considered to be that an on-axis entry was made into the lens, with zero vertical velocity. Table XV is submitted to show a typical page of computer results for this program.

TABLE XIV

TYPICAL DISCONTINUOUS PROGRAM FOR ELECTROSTATIC LENS

```
$JOB 2233-40031 H WAYNE WILLIS
  1      1 FORMAT(////,2X,5HAN = ,E10.4,3X,5HAK = ,E10.4,3X,4HT = E10.4,3X,6H
          1PTO = ,E10.4,3X,5HV = ,E10.4,3X,4HW = ,E10.4,3X,4HG = ,E10.4,/,2X
          2,4HH = ,E10.4,3X,5HDT = ,E10.4,3X,6HDPT = ,E10.4,3X,5HDV = ,E10.4,
          33X,5HVF = ,E10.4,3X,5HTF = ,E10.4)
  2      2 FORMAT(/,4X,I4,5X,6(E12.4),3X,E12.4,4X,E12.4)
  3      3 FORMAT(///,7X,1HM,10X,1HY,11X,1HS,9X,5HTHETA,5X,2HPT,9X,2HAX,9X,2H
          1AT,20X,3HPTS,12X,1HV)
  4      4 FORMAT(5X,E10.4)
  5        READ(5,4)AN,AK,T,PTO,VO,  W,G,H,DT,DPT,DV,VF,TF
  6      9 V=VO
  7        DVO=DV
  8     10 WRITE(6,1) AN,AK,T,PTO,V ,W,G,H,DT,DPT,DVO,VF,TF
  9     11 WRITE(6,3)
 10     12 AX=0.0
 11        PS=0.0
 12        PY=0.0
 13        PTS=0.0
 14     20 PT=PTO
 15        PT=PT-DPT
 16        X=V*T
 17        Z=X/(G+H)
 18        I=IFIX(Z)
 19        FI=FLOAT(I)
 20        D=Z-FI
 21        XL=(G+H)*D
 22        Q=XL-G
 23        L=1
 24        IF(Q.GT.0.0)L=2
 25        J=2*I+L
 26        M=1
 27        IF(X.LT.G) GOTO 60
 28     30 CALL EVOD(M,LOAD)
 29        IF(LOAD.EQ.2) GOTO 40
 30        R=G
 31        AX=(FLOAT(M+1)/2.0)*(G+H)-H
 32        GOTO 50
 33     40 R=H
 34        AX=(FLOAT(M)/2.0)*(G+H)
 35     50 AT=AX/V
 36        CALL EVOD(M,LOAD)
 37        IF(LOAD.EQ.2) GOTO 55
 38        PT=PT+DPT
 39        E=PT/R
 40        COM=(AN*AK*E*R)/(V**2)
 41        Y=(COM+PS)*R+PY
 42        S=2.0*COM+PS
 43        GOTO 56
 44     55 KOM=((AN*AK)/((V**2)*W))*(PT*R)
 45        SIM=((AN*AK)/((V**2)*W))*(DPT/H)*(R**2)
 46        Y=(KOM+PS)*R+(SIM*R)/3.0+PY
 47        S=2.0*KOM+SIM+PS
 48        PTS=PT+(DPT/H)*R
 49     56 THETA=ATAN(S)*57.29578
 50        IF(M.EQ.J) GOTO 70
 51        PY=Y
 52        PS=S
 53        M=M+1
 54        IF(M.EQ.J) GOTO 60
 55        GOTO 30

 56     60 R=XL
 57        IF(L.EQ.2) R=Q
 58        AX=AX+R
 59        GOTO 50
 60     70 WRITE(6,2)  M,Y,S,THETA,PT,AX,AT,PTS,V
 61        IF(V.GE.VF) GOTO 80
 62        IF(V.GE.1000.0)DVO= 10.0*DV
 63        V=V+DVO
 64        GOTO 12
 65     80 IF(AN.GE.5.0) GOTO 90
 66        AN=AN+1.0
 67        GOTO 9
 68     90 STOP
 69        END

 70        SUBROUTINE EVOD(M,LOAD)
 71        FM=(FLOAT(M))/2.0
 72        MO=IFIX(FM)
 73        F3=FLOAT(MO)
 74        F4=FM-F3
 75        IF(F4.GT.0.4) GOTO 200
 76        LOAD=2
 77        GOTO 300
 78    200 LOAD=1
 79    300 RETURN
 80        END

SENTRY
```

TABLE XV

SAMPLE COMPUTER OUTPUT FOR DISCONTINUOUS PROGRAM

AN = 0.5000E 01   AK = 0.1786E 07   T = 0.1000E-05   PTO = 0.3000E 01   V = 0.7000E 03   W = 0.4000E-01   G = 0.5000E-03
H = 0.1500E-02   DT = 0.1000E-05   DPT = 0.0000E 00   DV = 0.1000E 02   VF = 0.7000E 04   TF = 0.1000E-05

M	Y	S	THETA	PT	AX	AY	PTS	V
2	0.1252E-03	0.3060E 00	0.1701E 02	0.6000E 00	0.7000E-03	0.1000E-05	0.9579E 00	0.7000E 03
2	0.1247E-03	0.3007E 00	0.1673E 02	0.6000E 00	0.7100E-03	0.1000E-05	0.9758E 00	0.7100E 03
2	0.1242E-03	0.2957E 00	0.1647E 02	0.6000E 00	0.7200E-03	0.1000E-05	0.9937E 00	0.7200E 03
2	0.1237E-03	0.2910E 00	0.1623E 02	0.6000E 00	0.7300E-03	0.1000E-05	0.1012E 01	0.7300E 03
2	0.1232E-03	0.2866E 00	0.1599E 02	0.6000E 00	0.7400E-03	0.1000E-05	0.1029E 01	0.7400E 03
2	0.1228E-03	0.2825E 00	0.1578E 02	0.6000E 00	0.7500E-03	0.1000E-05	0.1047E 01	0.7500E 03
2	0.1223E-03	0.2787E 00	0.1557E 02	0.6000E 00	0.7600E-03	0.1000E-05	0.1065E 01	0.7600E 03
2	0.1219E-03	0.2750E 00	0.1538E 02	0.6000E 00	0.7700E-03	0.1000E-05	0.1083E 01	0.7700E 03
2	0.1215E-03	0.2716E 00	0.1520E 02	0.6000E 00	0.7800E-03	0.1000E-05	0.1101E 01	0.7800E 03
2	0.1211E-03	0.2685E 00	0.1503E 02	0.6000E 00	0.7900E-03	0.1000E-05	0.1119E 01	0.7900E 03
2	0.1207E-03	0.2655E 00	0.1487E 02	0.6000E 00	0.8000E-03	0.1000E-05	0.1137E 01	0.8000E 03
2	0.1204E-03	0.2627E 00	0.1472E 02	0.6000E 00	0.8100E-03	0.1000E-05	0.1155E 01	0.8100E 03
2	0.1200E-03	0.2600E 00	0.1458E 02	0.6000E 00	0.8200E-03	0.1000E-05	0.1173E 01	0.8200E 03
2	0.1197E-03	0.2576E 00	0.1444E 02	0.6000E 00	0.8300E-03	0.1000E-05	0.1191E 01	0.8300E 03
2	0.1194E-03	0.2553E 00	0.1432E 02	0.6000E 00	0.8400E-03	0.1000E-05	0.1208E 01	0.8400E 03
2	0.1191E-03	0.2531E 00	0.1420E 02	0.6000E 00	0.8500E-03	0.1000E-05	0.1226E 01	0.8500E 03
2	0.1189E-03	0.2511E 00	0.1410E 02	0.6000E 00	0.8600E-03	0.1000E-05	0.1244E 01	0.8600E 03
2	0.1186E-03	0.2492E 00	0.1399E 02	0.6000E 00	0.8700E-03	0.1000E-05	0.1262E 01	0.8700E 03
2	0.1184E-03	0.2475E 00	0.1390E 02	0.6000E 00	0.8800E-03	0.1000E-05	0.1280E 01	0.8800E 03
2	0.1182E-03	0.2458E 00	0.1381E 02	0.6000E 00	0.8900E-03	0.1000E-05	0.1298E 01	0.8900E 03
2	0.1180E-03	0.2443E 00	0.1373E 02	0.6000E 00	0.9000E-03	0.1000E-05	0.1316E 01	0.9000E 03
2	0.1178E-03	0.2428E 00	0.1365E 02	0.6000E 00	0.9100E-03	0.1000E-05	0.1334E 01	0.9100E 03
2	0.1177E-03	0.2415E 00	0.1358E 02	0.6000E 00	0.9200E-03	0.1000E-05	0.1352E 01	0.9200E 03
2	0.1176E-03	0.2403E 00	0.1351E 02	0.6000E 00	0.9300E-03	0.1000E-05	0.1369E 01	0.9300E 03

VITA[v]

Harold Wayne Willis

Candidate for the Degree of

Master of Science

Thesis: QUADRUPOLE MASS FILTER DESIGN AND CONSTRUCTION FOR PLASMA
ION ANALYSIS

Major Field: Physics

Biographical:

Personal Data: Born in Beaumont, Texas, October 1, 1942, the
eldest of three sons of Harold West and Mary McDonald
Willis. Married Eva Gerard Bomer on August 11, 1968.

Education: Attended grade school in Olympia, Washington,
Silsbee, Texas and Kountze, Texas; graduated from Kountze
High School, Kountze, Texas in May, 1960; received the
Bachelor of Science degree from the Lamar State College
of Technology in Beaumont, Texas in May, 1966; completed
the requirements for the Master of Science degree in
August, 1969.

Professional Experience: Laboratory technician and operator
assistant for the South Hampton Company of Houston, Texas
prior to completion of the requirements for the B. S.
degree; teaching assistant for the Department of Physics,
Lamar State College of Technology; President, Lamar
chapter of the American Institute of Physics, Beaumont,
Texas; Laboratory Assistant for the 1965 National Science
Foundation Summer Science Institute, Lamar Tech; recipient
of the National Science Foundation Summer Science In-
stitute appointment in Physical Science at the Howard
Payne College, Brownwood, Texas, 1959; Field Salesman for
the Periodical Publishing Company, Houston, Texas; Rodman
for the Geophysical Section of the Texaco Company, Inc.,
Gravity Part No. 105, Houston, Texas; Floorman for the
Carl Martin Oil Service Company, Houston, Texas; Teaching
Assistant for the Physics Department, Oklahoma State
University; Research Assistant for the Oklahoma State
University Research Foundation; Salutatorian of High
School graduating class; Member of the Lamar Freshman
Honor Society; Associate Member of Sigma Pi Sigma, Lamar

Chapter; Member of Sigma Pi Sigma, Oklahoma State Univer-
sity; Member of the Oklahoma State University Flying
Aggies; Junior Member of the American Association of
Physics Teachers; Member of the Oklahoma Academy of Science.